Method for Reducing Engine Cold Start Emissions from Transient Fueling in an Alternative Fueled Engine

Undergraduate Honors Thesis

Presented in Partial Fulfillment for Graduation with Distinction in the

Department of Mechanical Engineering at

The Ohio State University

Andrew W. Spiegel

The Ohio State University

2013

Defense Committee:

Professor Shawn Midlam-Mohler, Advisor

Professor Yann Guezennec

ABSTRACT

EcoCAR 2 is a three year competition among 15 North American Universities dedicated to reduce the negative environmental impact of a 2013 Chevy Malibu while maintaining standard vehicle operation. The planned E85 (85% ethanol and 15% gasoline) internal combustion engine for the vehicle produces harmful emissions during its cold startup. Previous research has shown that the majority of unwanted emissions from modern vehicles occur during engine cold starts. The inability to control the stoichiometric air fuel ratio from transient fuel dynamics as the engine warms is a major cause of these emissions. The purpose of this study was to create an engine control algorithm that compensates for the transient fuel dynamics during a cold start. The algorithm will be developed by determining fuel dynamic parameters describing the fuel evaporation time constant (τ) and fraction of liquid fuel entering the engine intake manifold (X). The fuel dynamic parameters are determined from comparing the exhaust air fuel ratio traces with step input perturbations of injected fuel. Because the fueling dynamics depend on temperature, engine speed, and manifold air pressure, the data from perturbation testing was collected over several engine speeds and manifold pressures during the engine's cold start. Lookup tables of τ and X parameters for different engine operating conditions were created and will be implemented into the engine control unit (ECU) to compensate the transient fueling. The research will help achieve the goals of the EcoCAR 2 competition to reduce the vehicle's environmental impact while maintaining standard operation. The procedure to create the algorithm can be implemented to control emissions of production E85 vehicles.

ACKNOWLEDGEMENTS

I would like to thank Dr. Shawn Midlam-Mohler for his advising during this project and willingness to help me complete this research even though things did not always turn out as planned. I would also like to thank fellow EcoCAR members Andrew Garcia and Jason Ward for giving me advice on various topics such as how to run the engine dynamometer. I would like to thank the other EcoCAR team members for their inclusion and support. Finally, I would like to thank the College of Engineering Honors Committee for the Undergraduate Research Scholarship.

TABLE OF CONTENTS

LIST OF FIGURES

Figure **Page**

LIST OF TABLES

Table **Page**

Chapter 1: INTRODUCTION

1.1 Background

Developing cleaner and more efficient vehicles is a pressing need for the future of the automotive industry. Since the late 1960s, the U.S. government has regulated harmful vehicle emissions for health and environmental concerns. Since 1980, the accumulation of increasingly rigorous emission control has reduced emissions by 49% in the United States [1]. Current Tier 2 vehicle emissions regulations and proposed Tier 3 regulations have accelerated automotive research in vehicle efficiency and emissions reduction technologies.

EcoCAR 2 is a three year student competition among select universities dedicated to promote research and new vehicle technology. EcoCAR 2's engineering goals are to increase fuel economy, decrease overall greenhouse gas emissions, and reduce tailpipe emissions of a production 2013 Chevy Malibu while retaining standard vehicle function and safety. Ohio State's EcoCAR 2 team is located at the Center for Automotive Research (CAR). Ohio State's team has decided to implement a parallel-series plug-in hybrid electric vehicle (PHEV) powertrain into the Chevy Malibu. The PHEV powertrain consists of a 1.8L Honda compressed natural gas (CNG) engine modified for E85 (85% ethanol and 15% gasoline) and two Parker-Hannifin electric machines powered by a battery pack. The advanced powertrain will be built to operate in charge depleting or charge sustaining modes depending on the battery charge and vehicle operation. During the charge sustaining mode, the engine will be required to power the vehicle or charge the batteries which leads to emissions production.

Ohio State's EcoCAR 2 team chose an E85 powered 1.8L Honda engine for several advantages. First, the engine has a high compression ratio of 12.5 to run on CNG. This higher

compression ratio improves the engine's fuel conversion efficiency. Second, E85 fuel has significant tailpipe emissions reductions in nitrous oxides (NO_x), hydrocarbons (HC), and carbon monoxide (CO) compared with similar gasoline engines [2]. Ethanol also has a greater octane rating than gasoline permitting the engine to run at a high compression ratio without inducing knock. Finally, the engine features several advanced features such as variable valve timing and adjustable intake runners for improved efficiency.

Part of the EcoCAR 2 competition includes the evaluation of vehicle emissions. Tailpipe emissions primarily consist of NO_x, HC, CO, nitrogen dioxide (N_2), carbon dioxide (CO_2), water (H_2O), hydrogen (H_2), and oxygen (O_2). The harmful tailpipe emissions of NOx, HC, and CO, however, are the emissions of most interest. Most modern vehicles feature a three-way catalytic converter on the vehicle's exhaust and control methods for air and fuel flow to reduce these emissions.

1.2 Motivation

Automobiles have often harmed the environment by polluting the air. Vehicles that run on alternative fuels such as E85 are gaining more widespread attention as practical fueling options for lower emissions. Although E85 is cleaner than gasoline, it still combusts to form the same harmful emissions. E85, like gasoline, experiences transient fuel dynamics as the engine warms to a steady temperature. An accurate compensator for these fuel dynamics will make E85 a more desirable fuel for lower emissions. Efforts that successfully reduce emissions from E85 powered vehicles may promote it and other alternative fueled vehicles for a healthier environment.

1.3 Purpose of Research

The purpose of this research is to develop an ECU control algorithm to compensate for the transient fueling dynamics of an E85 powered engine during cold starts. Research has shown that up to 80% of HC and CO emissions occur during the engine's cold start process [3]. The two primary reasons for high cold start emissions include inefficient catalytic functioning at cold conditions and inaccurate air fuel ratio (AFR) control. The research will focus on strict cold start AFR control by developing an algorithm to accurately predict fuel dynamics of the Honda engine at various operating conditions.

Chapter 2: LITERATURE REVIEW

2.1 Engine Emissions

Regulating automotive emissions has been of increasing significance since the late 1960's. As specific tailpipe emissions have been found to cause a variety of health and environmental issues, further regulations continue to be implemented. Currently regulated harmful vehicle emissions in the United States include CO, NO_x, non-methane organic gasses (NMOG), and particulate matter (PM).

The main focus of this research is to reduce the criteria gas emissions of CO, NO_x, and unburned and partially burned HC. Particulate matter from spark ignition (SI) engines is generally ignored as they are much less in comparison to compression ignition (CI) engines. The methods of SI engine pollutant formation are shown in Figure 2:1 below. CO is formed from the incomplete combustion of excess hydrocarbons with air and from high temperature combustion. NO_x is caused primarily from reacting N_2 and O_2 species at high cylinder temperatures. NMOG consists of total hydrocarbons (THC) and organic gasses leaving the tailpipe excluding methane [4]. Hydrocarbon emissions come from partial burning of fuel or from fuel that escapes the combustion process in the cylinder.

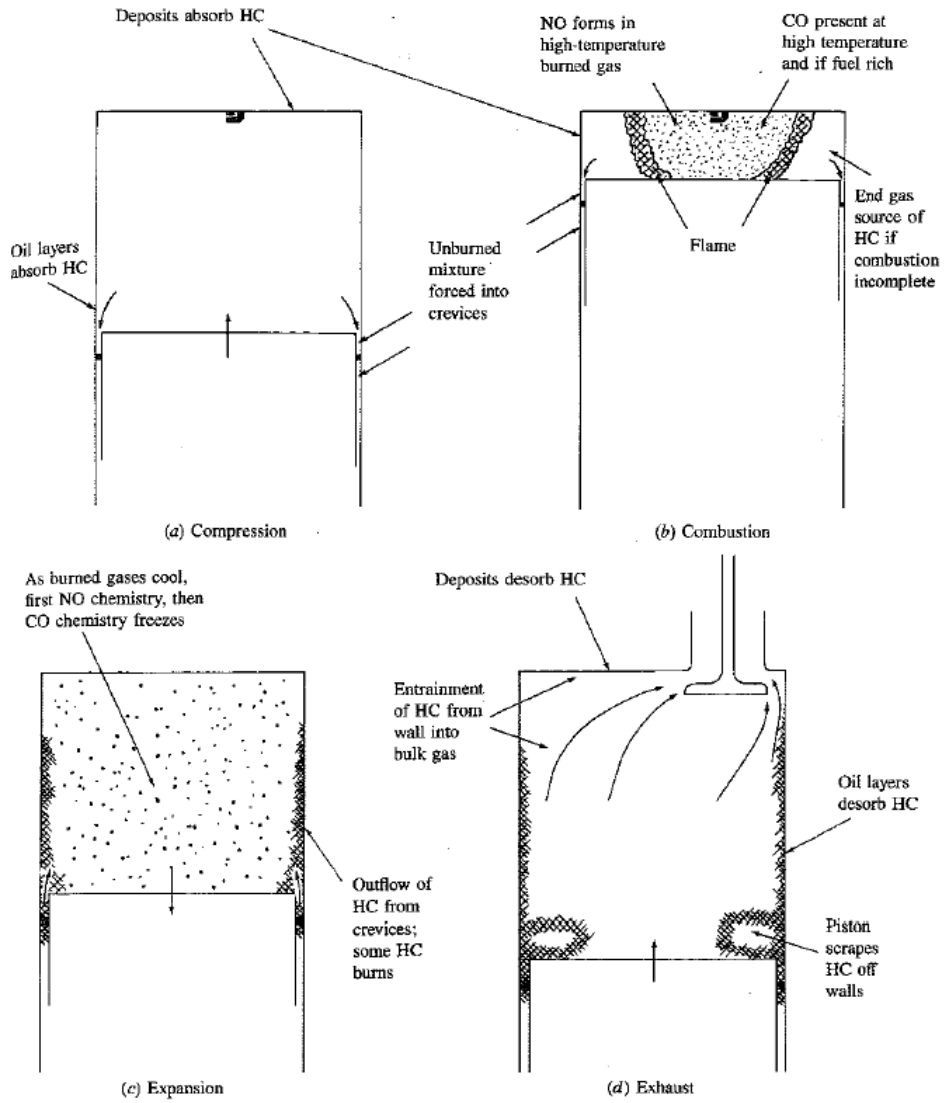

Figure 2:1: HC, NO, and CO Engine Pollutant Formation [5]

2.2 AFR Control

A common method engineers use to reduce HC and CO emissions is AFR control. The air fuel ratio is described as the parts of air divided by the parts of fuel as shown in Equation 2.1. The inverse of the AFR is the fuel air ratio as described by equation 2.2. The optimum reduction in HC and CO emissions reductions occur close to stoichiometric conditions. Stoichiometry describes the ideal condition where the oxygen in air combusts completely with fuel yielding

only CO_2 and H_2O. The stoichiometric air fuel ratio of E85 fuel is 9.87. The AFR and fuel air ratio equations can be normalized by the stoichiometric AFR or fuel air ratio to give the relative air fuel ratio and the equivalence ratio (EQR) equations 2.3 and 2.4. The relative AFR and equivalence ratios are used to describe how relatively lean or rich the air fuel mixture is in an engine. For example, an equivalence ratio greater than 1 describes a rich mixture (excess fuel) and an equivalence ratio less than 1 describes a lean mixture (excess air).

$$AFR = \frac{\dot{m}_a}{\dot{m}_f} \tag{2.1}$$

$$Fuel\ Air\ Ratio = \frac{\dot{m}_f}{\dot{m}_a} \tag{2.2}$$

$$\lambda = \frac{\left(\frac{A}{F}\right)act}{\left(\frac{A}{F}\right)_{stoic}} \tag{2.3}$$

$$\Phi = \frac{\left(\frac{F}{A}\right)act}{\left(\frac{F}{A}\right)_{stoic}} \tag{2.4}$$

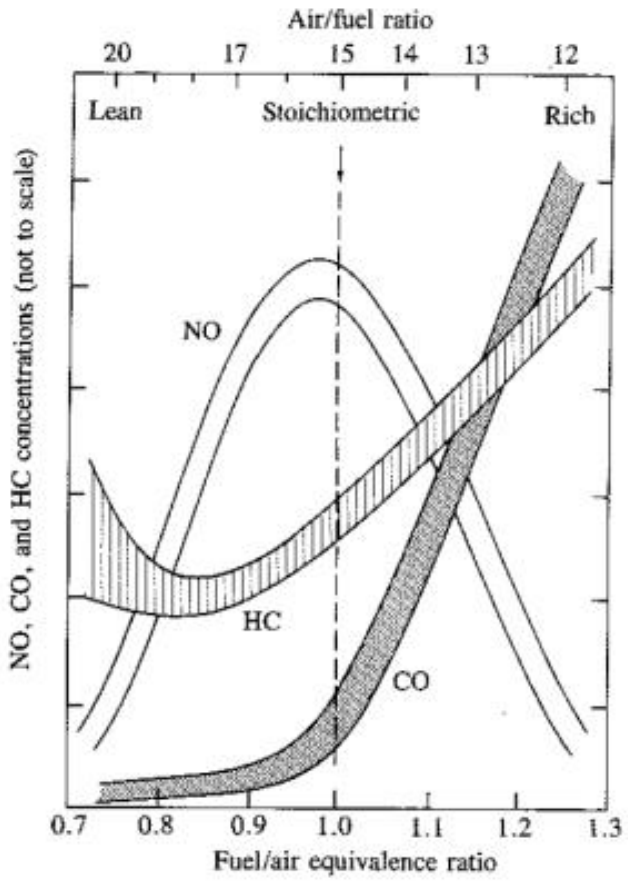

Figure 2:2: Common Emissions vs. AFR [5]

Figure 2:2 above displays emissions trends vs. AFR. As noted in the figure, generally lower CO and HC occur close to stoichiometry. NO, however, reaches a maximum slightly lean of stoichiometry. Car manufacturers permit the large amount of NO emissions in return for lower HC and CO emissions as well as higher brake torque. The three-way catalyst is the primary system used for reducing NO emissions.

2.3 Cold Start

The engine start-up process from a relatively cool temperature to its steady operating temperature has been known to cause high emissions. This process, known as an engine cold start, is defined as an engine start from ambient room temperatures around 20-30°C or lower [6].

Until the engine reaches a controlled steady state temperature after 1 to 2 minutes, the emission output will be of much greater magnitude than any other time of engine operation. Two primary causes of cold start emissions are (1) the catalyst's low performance until its "light-off" temperature around 300°C and (2) unsteady AFR control from transient fuel dynamics [6].

2.3.1 Three-Way Catalyst

A three-way catalytic converter is a device commonly found in vehicle aftertreatment systems to reduce harmful air pollutants. The catalyst's primary task is to convert three harmful pollutants of HC, NO_x, and CO into less dangerous H_2O, N_2, and CO_2. The catalyst converts these three pollutants by the reduction of NO_x into N_2 and O_2 and the oxidation of HC and CO into H_2O and CO_2. The five primary reaction equations are listed in equations 2.5 through 2.9 [6].

$$2HC + \frac{5}{2}O_2 \longrightarrow 2CO_2 + H_2O \tag{2.5}$$

$$CO + \frac{1}{2}O_2 \longrightarrow CO_2 \tag{2.6}$$

$$NO + CO \longrightarrow CO_2 + \frac{1}{2}N_2 \tag{2.7}$$

$$10NO + 4HC \longrightarrow 4CO_2 + 2H_2O + 5N_2 \tag{2.8}$$

$$NO + H_2 \longrightarrow \frac{1}{2}N_2 + H_2O \tag{2.9}$$

The efficiency of a catalytic converter has been found to vary against temperature. The "light-off" temperature is a parameter used to describe when a catalyst can successfully treat emissions. The "light-off" temperature occurs once the catalytic efficiency reaches 50% for a

particular emission. Figure 2:3 below shows a representation of catalytic efficiency vs. temperature as well as “light-off” temperature locations for CO and HC.

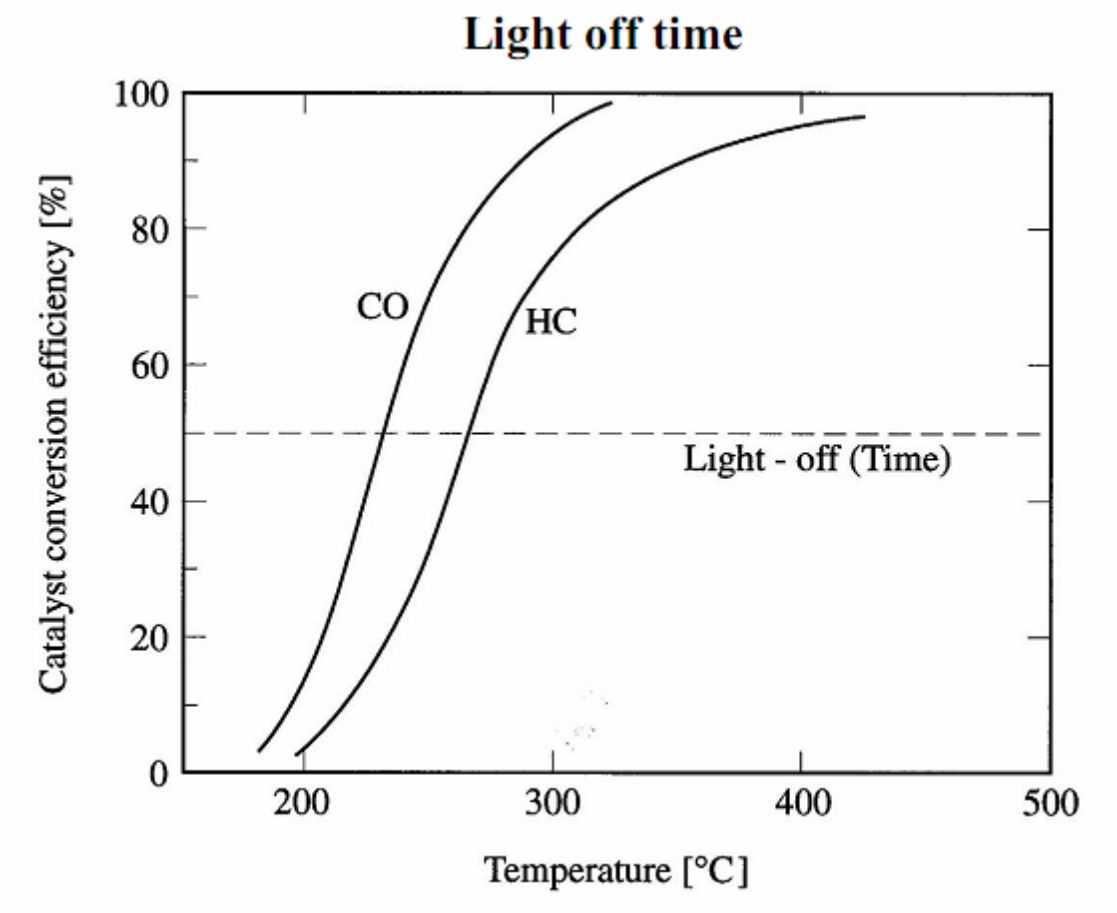

Figure 2:3: Catalyst Efficiency vs. Temperature [5]

During an engine cold start, the cold catalyst bypasses harmful emissions. In order to compensate for the catalyst’s ineffectiveness, several methods are utilized to prevent catalytic inefficiency. One common method is using a hydrocarbon absorber which traps hydrocarbons until the catalyst reaches “light-off” temperature. Another method is the use of a close-coupled catalyst. The design of a close-coupled catalyst involves placing the catalyst in close proximity to or within the exhaust manifold. A final method to compensate for a cold catalyst is using an electrically heated catalyst (EHC). An EHC works by sending an electrical current through a foil

structure which transfers heat to gasses within the EHC. These warm gasses flow down the exhaust to heat the main catalyst [7].

2.3.1.1 Electrically Heated Catalyst

The EcoCAR 2 team has decided to implement an electrically heated catalyst on the 2013 Chevy Malibu. The catalyst is an Emicat® EHC integrated with an Emicat® Series 6d catalyst [7]. The catalyst was chosen for the EcoCAR 2 competition because it had successfully reduced select cold start emissions by 80-90% on the previous EcoCAR [7]. The implementation of the EHC leaves transient fuel dynamics as the remaining primary cause of cold start emissions.

2.3.2 Transient Fuel Dynamics

In modern engines, fuel injectors are used to inject fuel with precise timing into the intake manifold. The fuel enters the engine's intake manifold close to the intake valve of the cylinder. The fuel enters the manifold as a partially evaporated and partially liquid mixture. The evaporated fuel enters into the cylinder immediately when the intake valve opens. The liquid fuel, however, forms fuel puddles in the intake manifold. The manifold close to the engine cylinder is warm and causes the liquid fuel to evaporate over time. Both the rate at which fuel evaporates and the composition of fuel entering the manifold depend on several engine operating conditions including engine temperature.

During the engine cold start process, the fuel rate that actually enters the cylinder changes as the engine warms. Because the fuel rate that enters the cylinder is not the commanded fuel rate of the injectors, the air fuel ratio cannot be accurately controlled to achieve stoichiometry. The changing fuel rates that actually enter into the engine cylinder during cold starts are what define transient fuel dynamics.

2.3.2.1 Aquino Model

Aquino was the first to create a model in 1981 to describe the physical nature behind transient fueling. His model incorporates an evaporation time constant, τ, and a variable to describe the fraction of liquid fuel entering the cylinder, X. He applied the conservation of mass to describe the fuel puddle or "film" in the intake as shown in equation 2.10 [8]. The rate of vaporized fuel was described with the X parameter in equation 2.11 [8]. The actual rate of fuel entering the cylinder is a combination of equation 2.11 and the fuel rate leaving the puddle to create equation 2.12 [8]. A pictorial representation of the Aquino or τ-X model is shown in Figure 2:4. His model is still implemented in many transient fuel compensation strategies including this research.

$$\frac{dm_p}{dt} = \dot{m}_\iota - \dot{m}_o = X\dot{m_{inJ}} - \frac{1}{\tau}m_p \tag{2.10}$$

$$\dot{m}_v = (1 - X)\dot{m_{inJ}} \tag{2.11}$$

$$\dot{m_{cyl}} = (1 - X)\dot{m_{inJ}} + \frac{1}{\tau}m_p \tag{2.12}$$

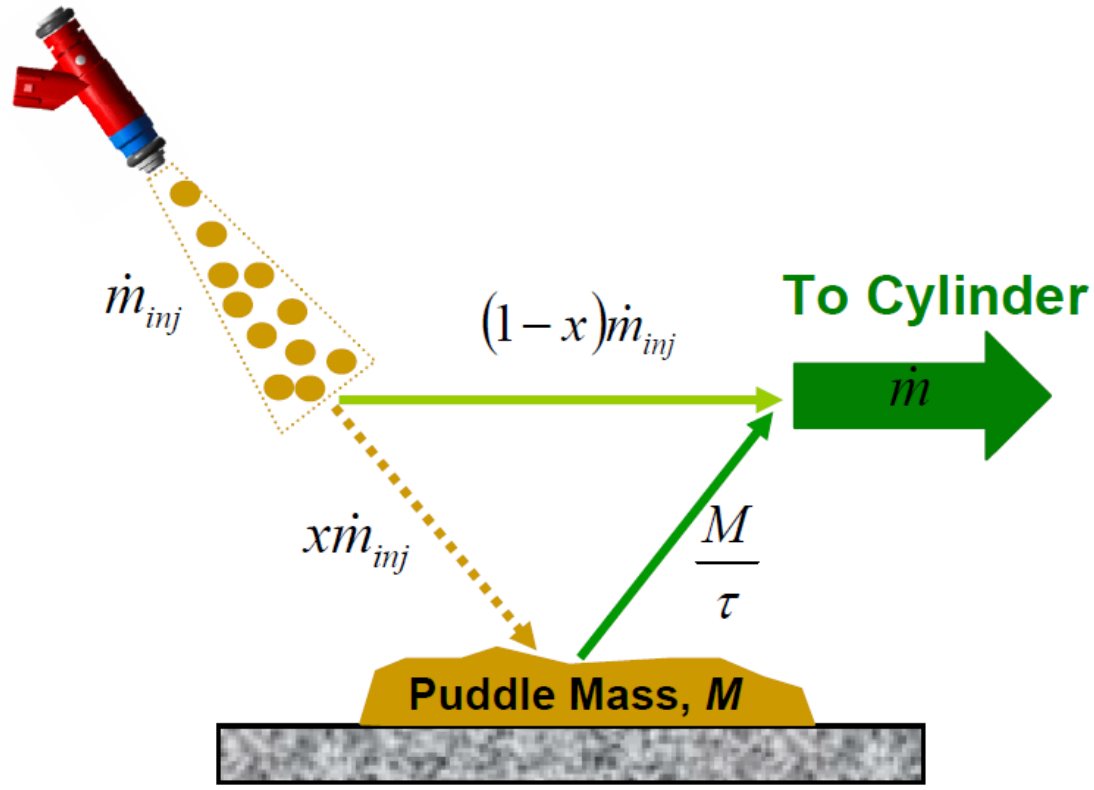

Figure 2:4: Aquino Model [9]

2.3.2.2 Compensation Methods

In order to compensate for the fuel dynamics entering the engine, a method must be used to determine τ and X parameters as a function of engine operation characteristics. Once τ and X are determined, the two parameters can be utilized to determine the correct injected fuel rate required to maintain a stoichiometric AFR at different operating conditions.

Both τ and X parameters have been shown to depend on the type of fuel, engine temperature, engine speed, and manifold air pressure (MAP) [10]. Figure 2:5 shows how various contents of ethanol change the X parameter. τ and X tend to decrease as a function of engine coolant temperature (ECT) and engine speed as represented in Figures 2:6 and 2:7. Additional studies have shown that an increasing MAP increases X and decreases τ [11].

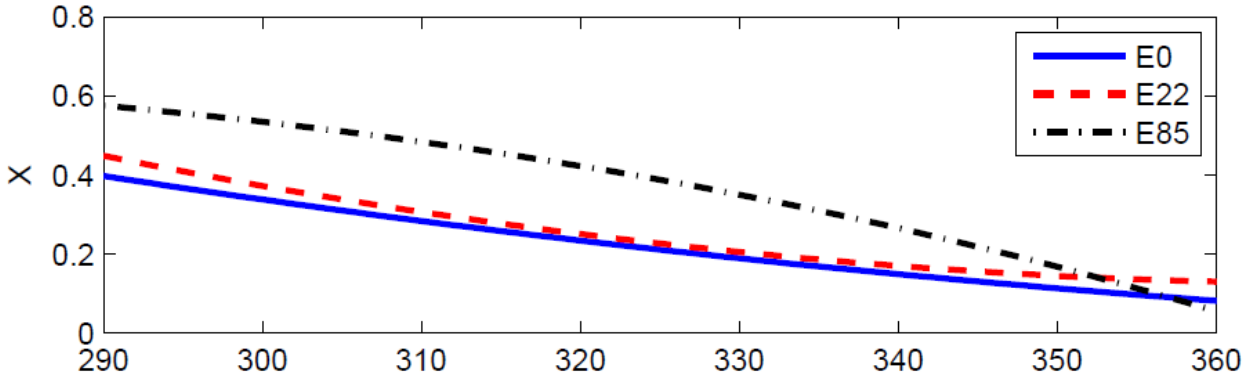

Figure 2:5: X vs. Engine Coolant Temperature for Various Ethanol Content [12]

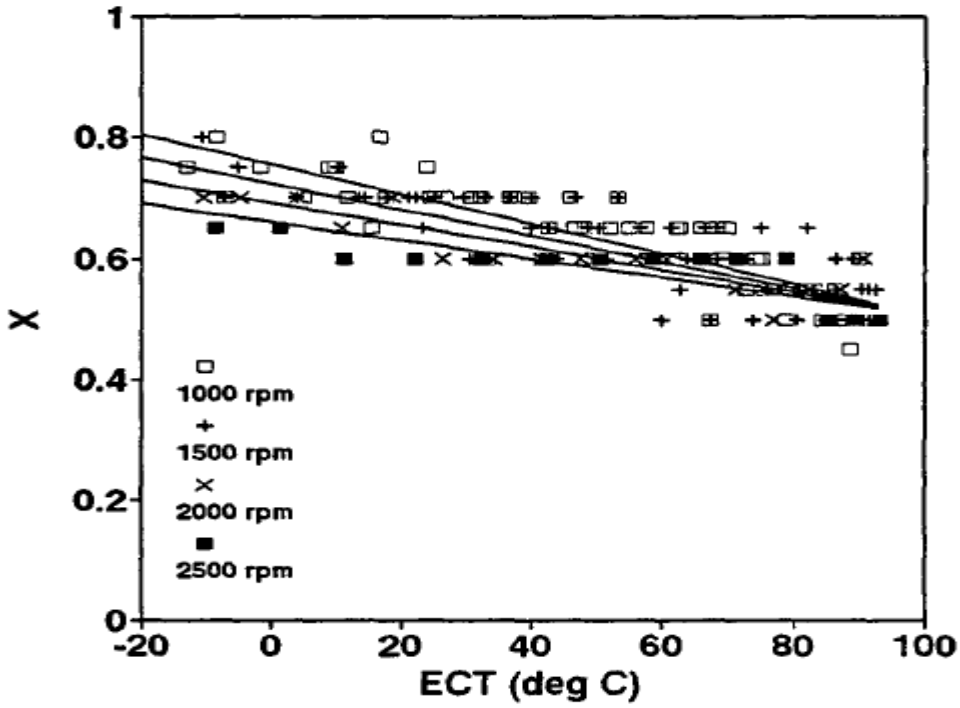

Figure 2:6: X vs. Engine Coolant Temperature and RPM [13]

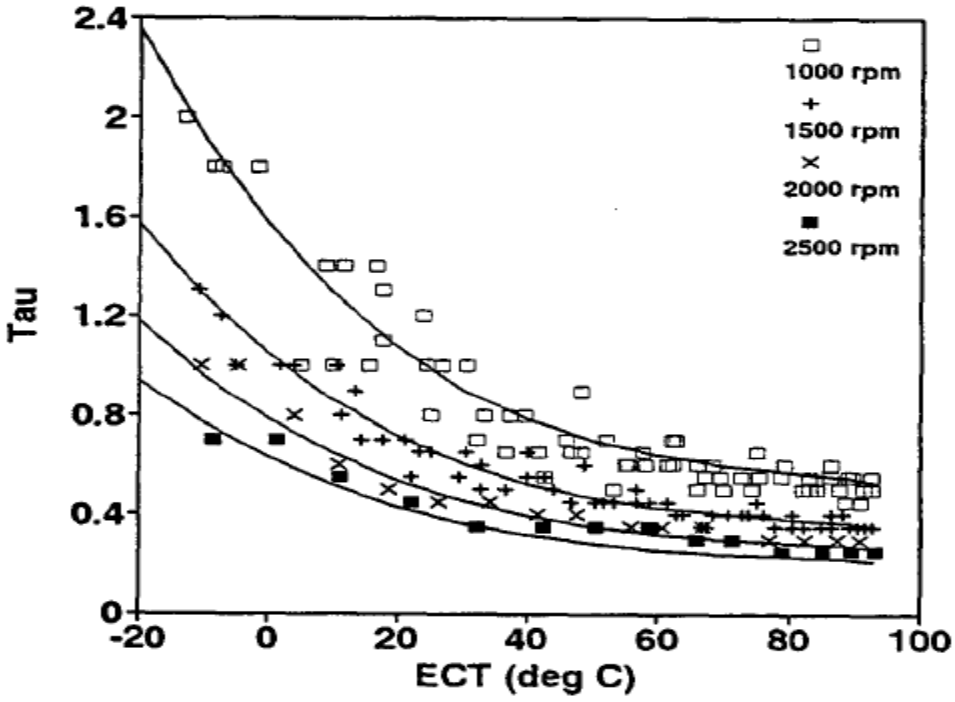

Figure 2:7: τ vs. Engine Coolant Temperature and RPM [13]

In order to determine τ and X, a method must be implemented to retrieve data from the fueling dynamics. One of the most common methods to determine the parameters is a fuel perturbation method [10]. The fuel perturbation method involves controlling the fuel injectors to inject square waves during a cold start. EQR response data from a pre-catalyst oxygen sensor will show how the fuel dynamics affect the fuel entering the cylinder. Figure 2:8 displays the injector fuel rate and the EQR response data from a fuel perturbation test.

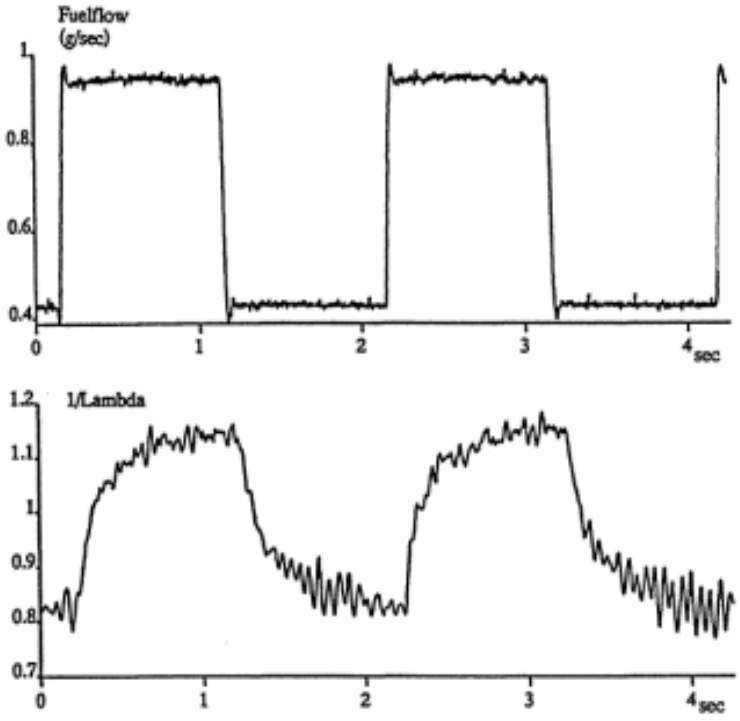

Figure 2:8: Sample Perturbation Test [10]

2.3.3 Heated Fuel Injectors

A relatively new method for reducing cold start emissions involves using heated fuel injectors. Heated fuel injectors were designed specifically for vehicles with ethanol based fuels. These fuels have a low flash point temperature which is the lowest temperature a fuel can be vaporized for combustion. Ethanol based fuels usually require rich fueling during cold start to ensure proper start-up because pure ethanol has a flash point temperature of 12°C [14]. This rich fueling causes higher HC and CO emissions during cold starts. When using heated fuel injectors, the rich fueling is not required, and this results in HC and CO emission reduction up to 40% [14].

2.4 Summary

Regulating vehicle emissions is a primary concern for reducing their harmful effects on human health and the environment. The three criteria gas emissions of vehicle exhaust are CO,

NO_x, and HC. The most common method for reducing these emissions on vehicles is through the use of air fuel ratio control in combination with a three-way catalyst.

Cold start emissions represent a significant portion of vehicle emissions. The primary causes of cold start emissions are low catalytic converter performance at low temperatures and unsteady air fuel ratio control from fuel dynamics. The EcoCAR 2 team is using an EHC to compensate for the catalyst's low efficiency at start-up. This research will focus on creating an algorithm to control the fuel dynamics described by the Aquino model. If time permits, HFIs will also be implemented to help further reduce cold start emissions relating to ethanol based fuels.

Chapter 3: EXPERIMENTAL EQUIPMENT

All experiments for this research were performed at the Center for Automotive Research. The experiments occurred with a four-quadrant, 200 hp DC dynamometer from a safe control test cell. The dynamometer was used with constant speed control during engine testing. The engine used was a 1.8L, 4-cylinder Honda engine converted to run on E85 fuel. The engine's Woodward engine control unit (ECU) in connection with ETAS INCA software was used to collect desired engine data.

3.1 Engine Instrumentation

The engine is monitored by its control unit with numerous sensors. When desired, the data from these sensors can be sent from the ECU for analysis. Table 3:1 displays the sensors used in experiments. ETAS INCA software was the data acquisition system used to obtain readings from the ECU and control the experiments. Figures 3:1 and 3:2 show the location of selected engine sensors used in data acquisition.

Table 3:1: List of Engine Sensors Used

Engine Sensors	
1	Pre-CAT UEGO Sensor
2	Fuel Sensor
3	Mass Air Flow Sensor
4	Manifold Air Pressure Sensor
5	Engine Coolant Temperature Sensor
6	Engine Speed Sensor

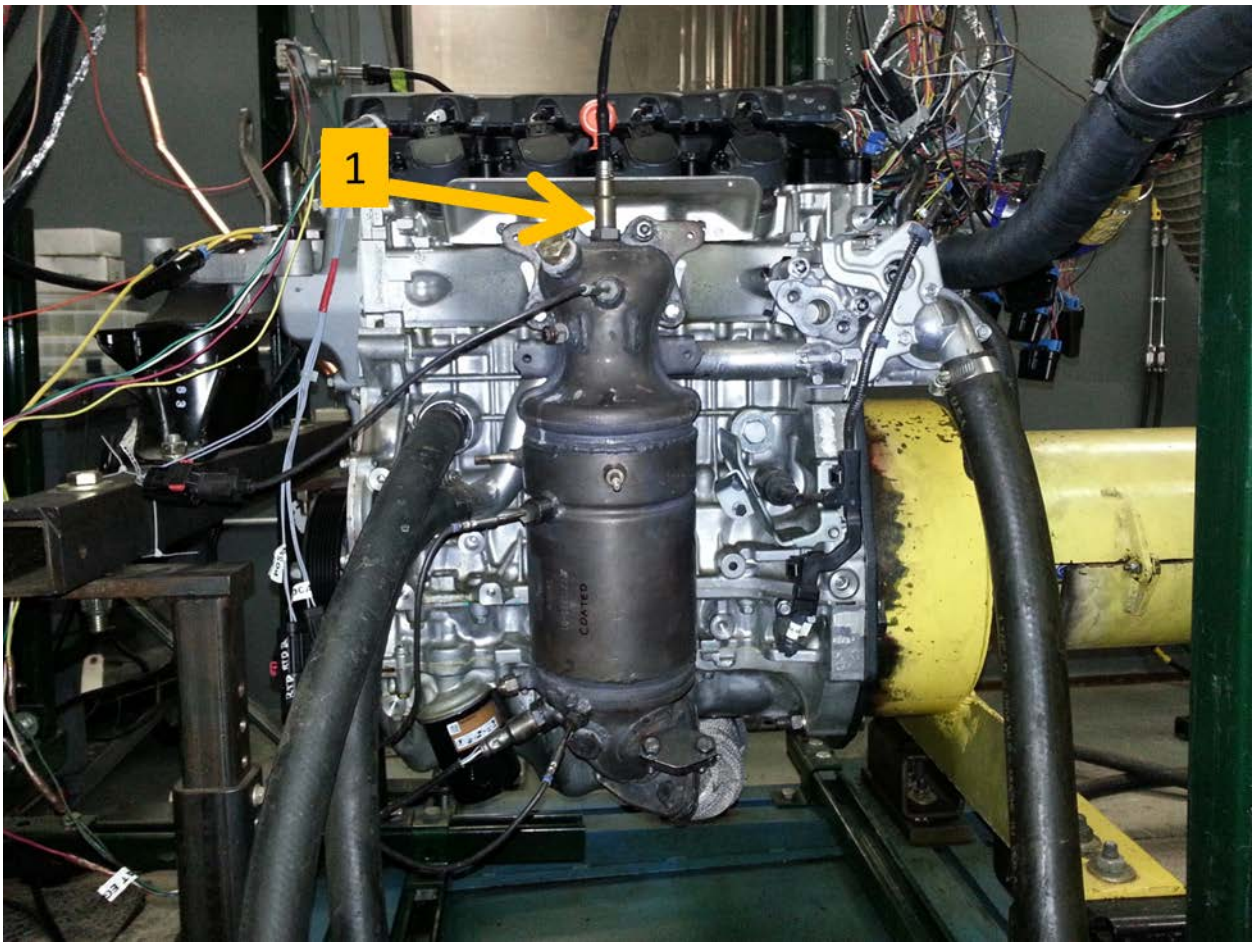

Figure 3:1: Location of Pre-Cat Sensor

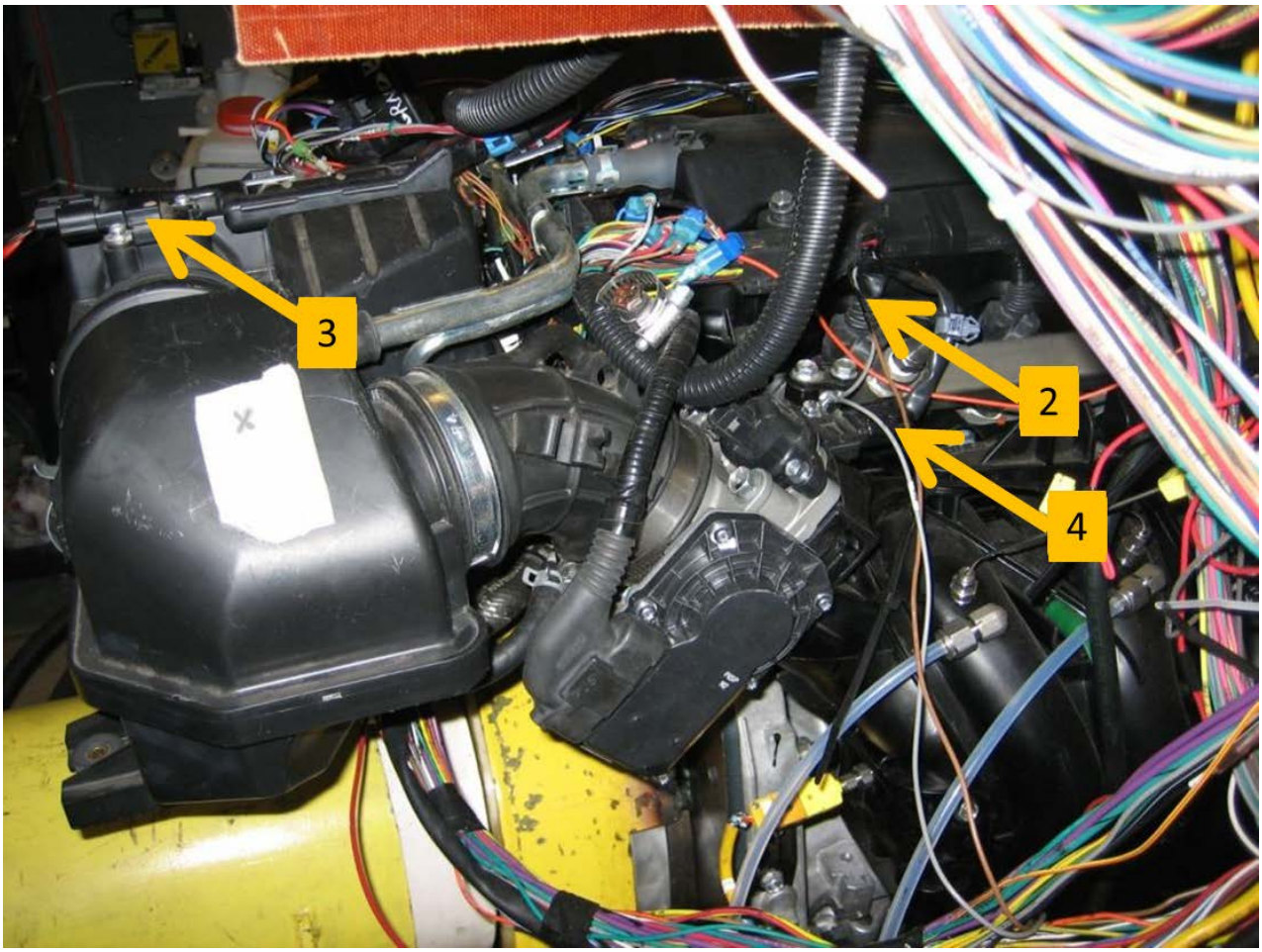

Figure 3:2: Location of Fuel, MAF, and MAP Sensors [15]

3.2 Dynamometer

The engine dynamometer used in the experimental setup is a 200 hp, 4-quadrant, DC dynamometer. The dynamometer has control options for constant speed or constant torque. The experiments performed for this research used constant speed control at 1000, 2000, and 3000 RPM. The dynamometer tests were controlled from a test cell located next to a sealed engine bay with the dynamometer and engine.

3.3 Data Acquisition and Software

ETAS INCA software was used to collect sensor data from the Woodward ECU. The INCA software allows the user to both visually observe and collect desired data from a workspace on a laptop. The INCA software was used to initialize engine operation after the engine bay had been prepared for testing. Control features in the INCA software permit the user to modify engine operation parameters such as throttle percentage or fuel flow rate. The fuel perturbation testing in this experiment was controlled and initialized through INCA.

The software developed to control the engine was created in MATLAB's Simulink with both Simulink and MotoHawk models. MotoHawk is an application which permits a user to develop block diagram engine models in Simulink. The created models can be uploaded onto the Woodward ECU with Mototune flash programming in a short time frame.

Chapter 4: EXPERIMENTAL PROCEDURE

4.1 Testing Methodology

To accurately determine the τ and X parameters of the Aquino model, a testing procedure must be implemented to clearly observe and determine the fueling dynamics. The most common method for collecting fuel dynamics data is through the use of the perturbation method described in section 2.3.2.2. This method is used to determine τ and X parameters from pre-catalyst EQR traces. Figures 4:1 and 4:2 below demonstrate how the τ and X parameters affect the EQR response data for up and down perturbations. The fraction of evaporated fuel (1-X) results in a close to instantaneous "jump" in EQR. The τ parameter is then determined from the approximate 1st order response in EQR until it reaches a steady state value.

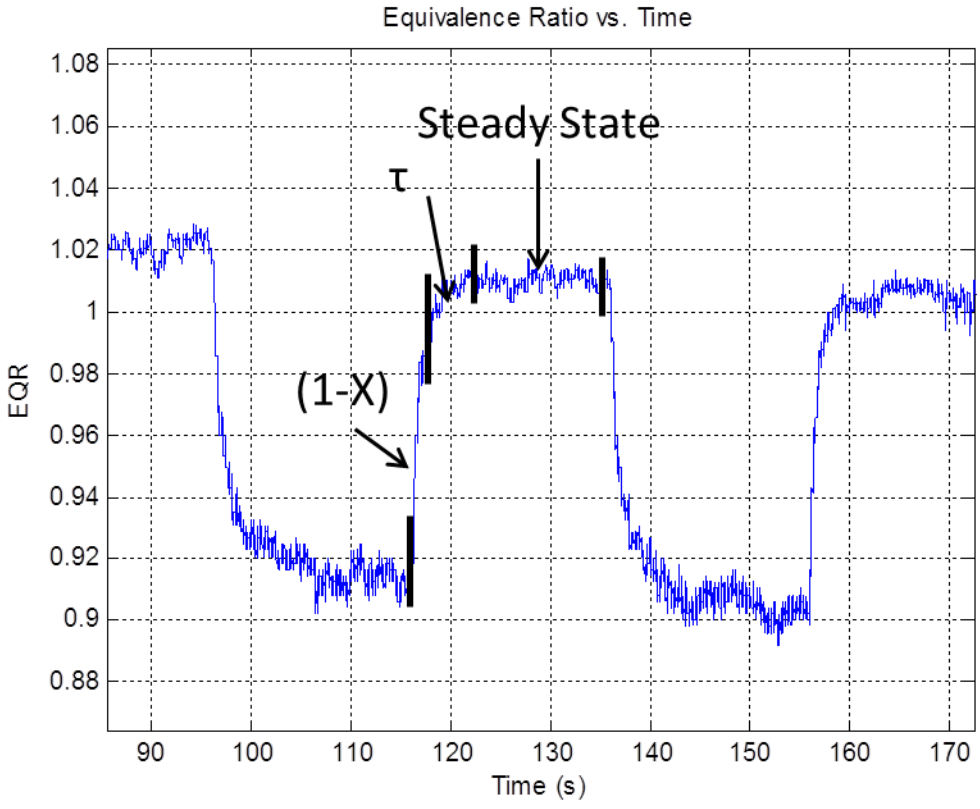

Figure 4:1: Representation of Fuel Dynamics Parameters in Up Perturbation

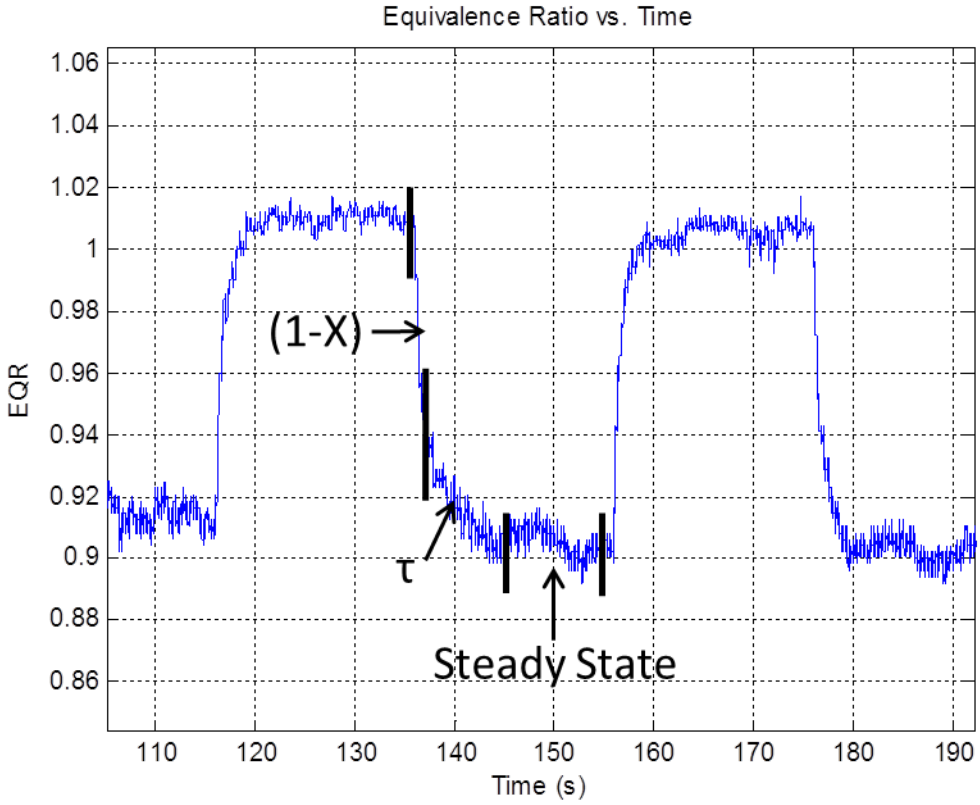

Figure 4:2: Representation of Fuel Dynamic Parameters in Down Perturbation

To make a greater impact on emissions reduction, a "map" of τ and X data is desired over a range of common engine operating conditions. It is known that τ and X are functions of engine speed, MAP, and temperature. The τ and X parameters were decided to be determined at a set engine speed and MAP from an engine cold start near room temperature until the steady state operating temperature of 80°C. Engine speeds of 1000 RPM, 2000 RPM, and 3000 RPM were used vs. MAPs of 30 kPa, 60 kPa, and wide open throttle (WOT) for nine total engine tests. The MAP for the low load and 1000 RPM case was set to approximately 40 kPa instead of 30 kPa to ensure that the engine would not stall.

4.2 Data Collection

The software in the engine's ECU had a previously created model for fuel perturbation testing. The user has the ability to enable the model and determine the frequency and the percent amplitude of square wave fuel injection above and below stoichiometry. Figures 9:1 and 9:2 in Appendix A show the fuel perturbation model in the engine code and within the subsystem.

It was determined that the fuel perturbations were to be set at ±5% of the stoichiometric air fuel ratio with a frequency of 0.05 Hz for 20 second perturbations. The 5% air fuel ratio perturbation was used because limiting emissions during experimentation was desired and larger perturbation amplitudes values tend to create nonlinearities [10]. The frequency was set to 0.05 Hz to ensure that the fuel dynamics reached steady state by the end of each perturbation especially in low speed and low MAP cases.

4.3 Experiment Results

Figures 4:3 through 4:11 display segments of the normalized fuel injected and EQR from the nine engine experiments. The normalized fuel injection rate was plotted by dividing by the mean fuel injected rate. The fuel injection was not consistently from 0.95 to 1.05 in Figure 4:6 because the mean value was high from large fuel enrichment spikes captured in the beginning. Figure 9:3 in Appendix B shows the entire perturbation test with these spikes.

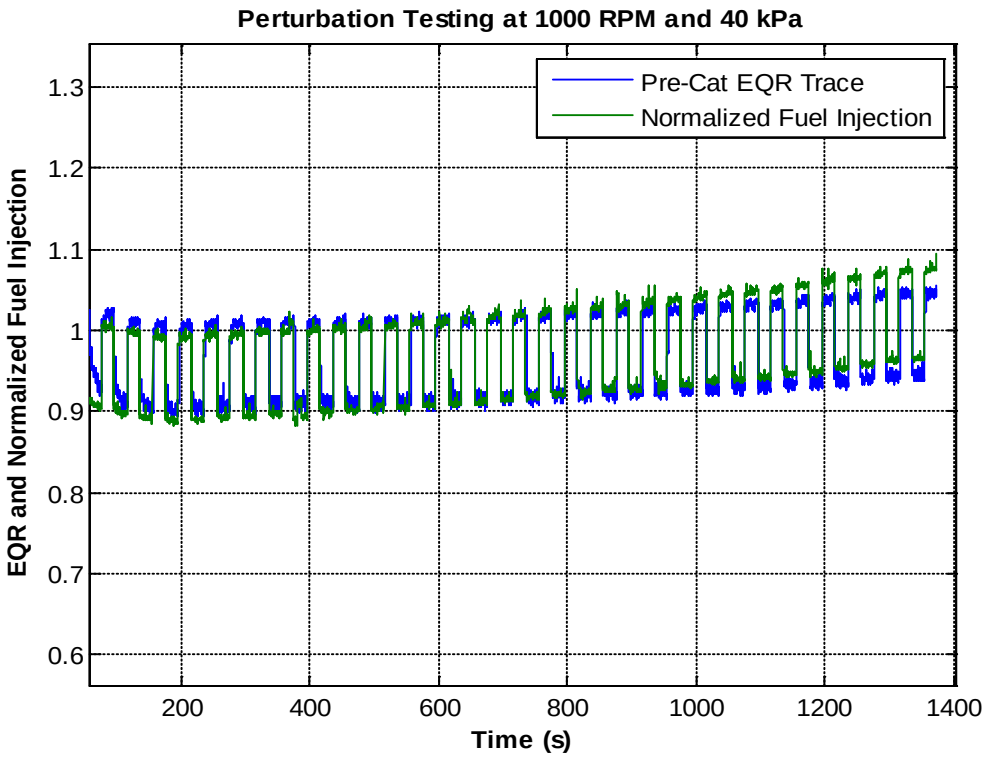

Figure 4:3: 1000 RPM and 40kPa Results

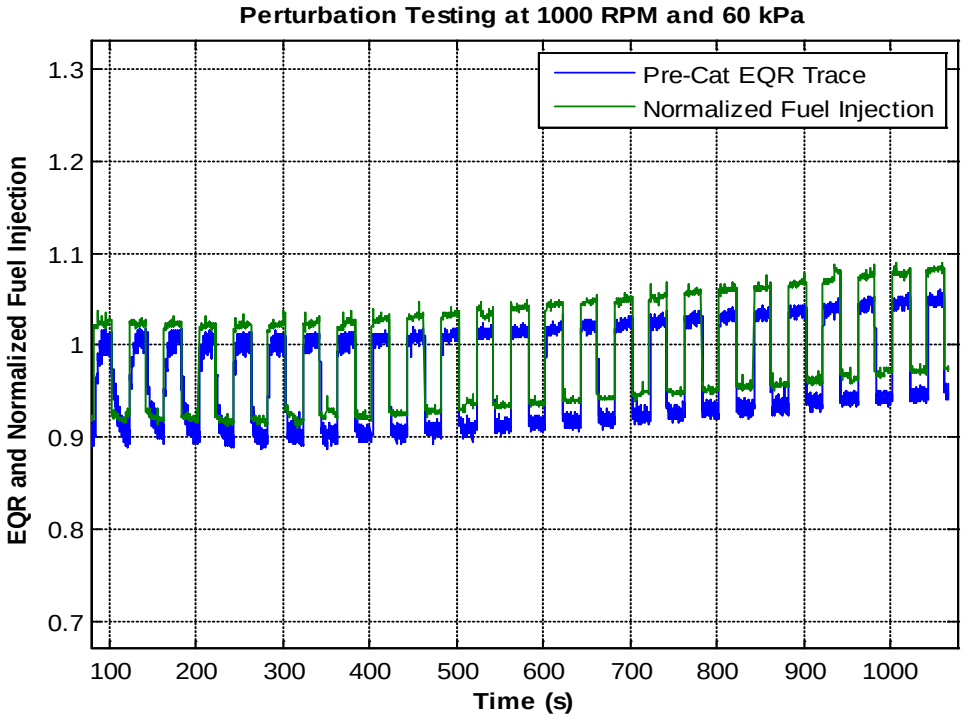

Figure 4:4: 1000 RPM and 60kPa Results

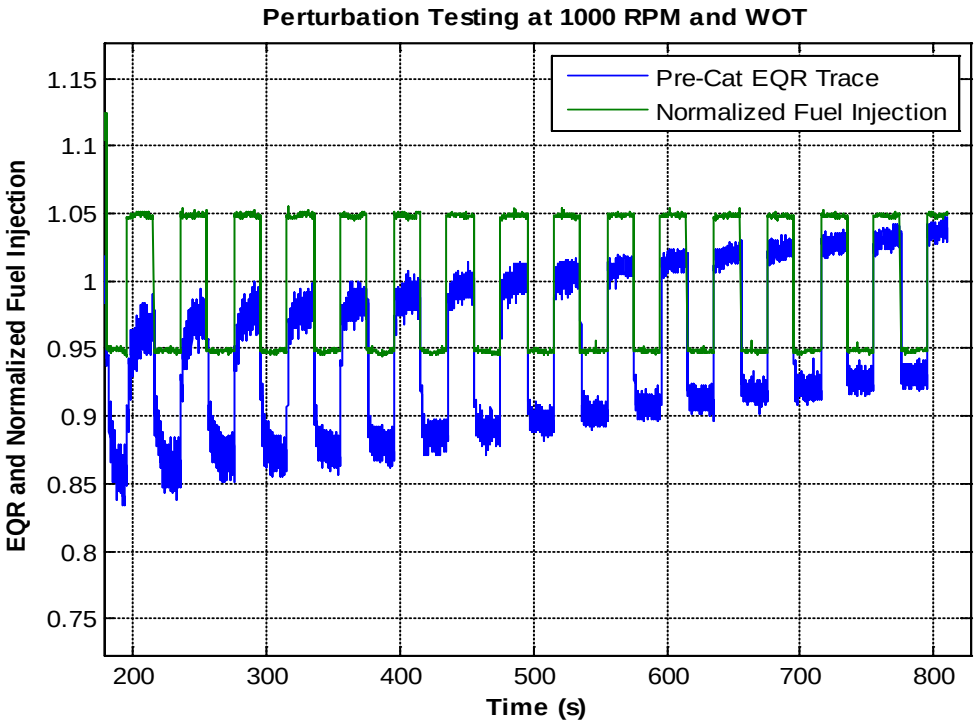

Figure 4:5: 1000 RPM and WOT Results

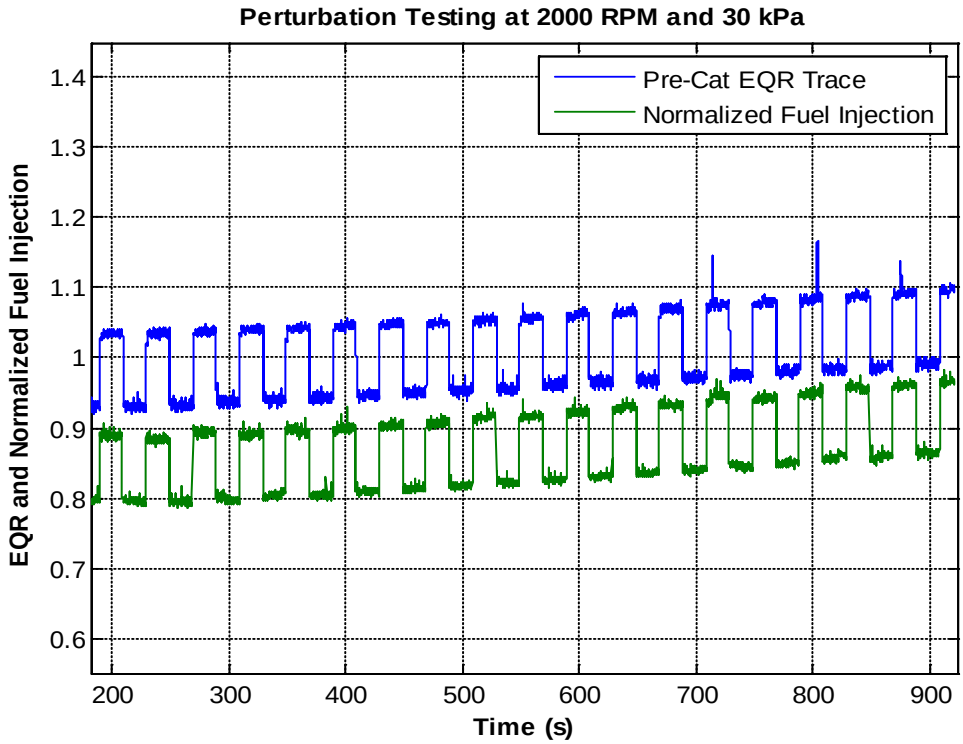

Figure 4:6: 2000 RPM and 30kPa Results

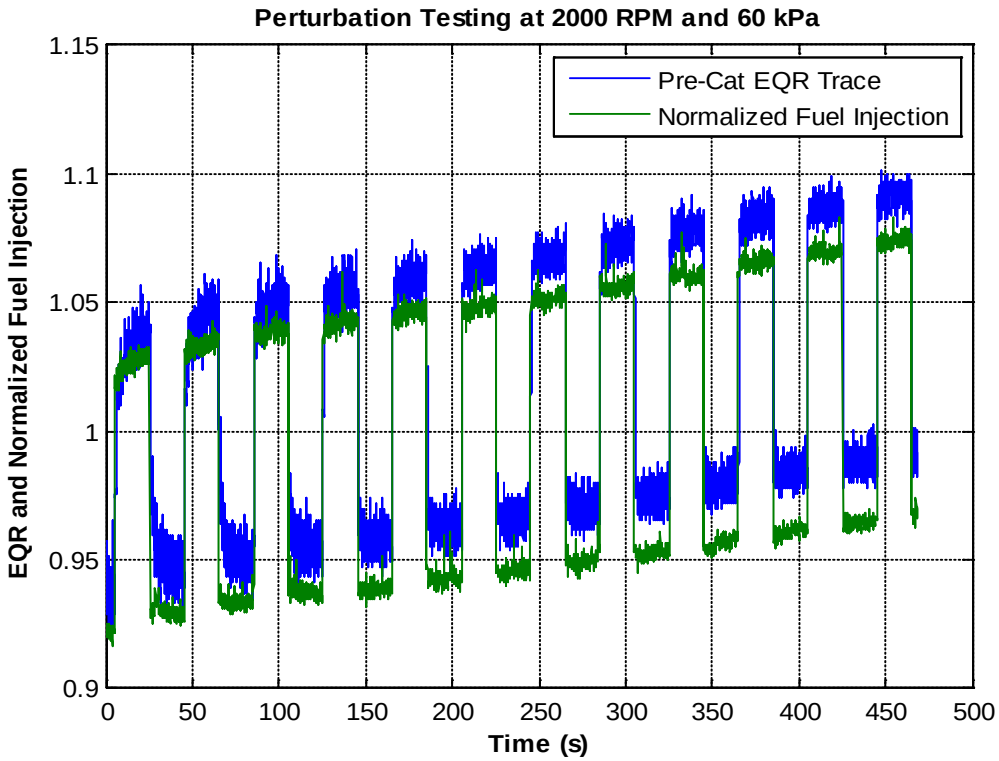

Figure 4:7: 2000 RPM and 60kPa Results

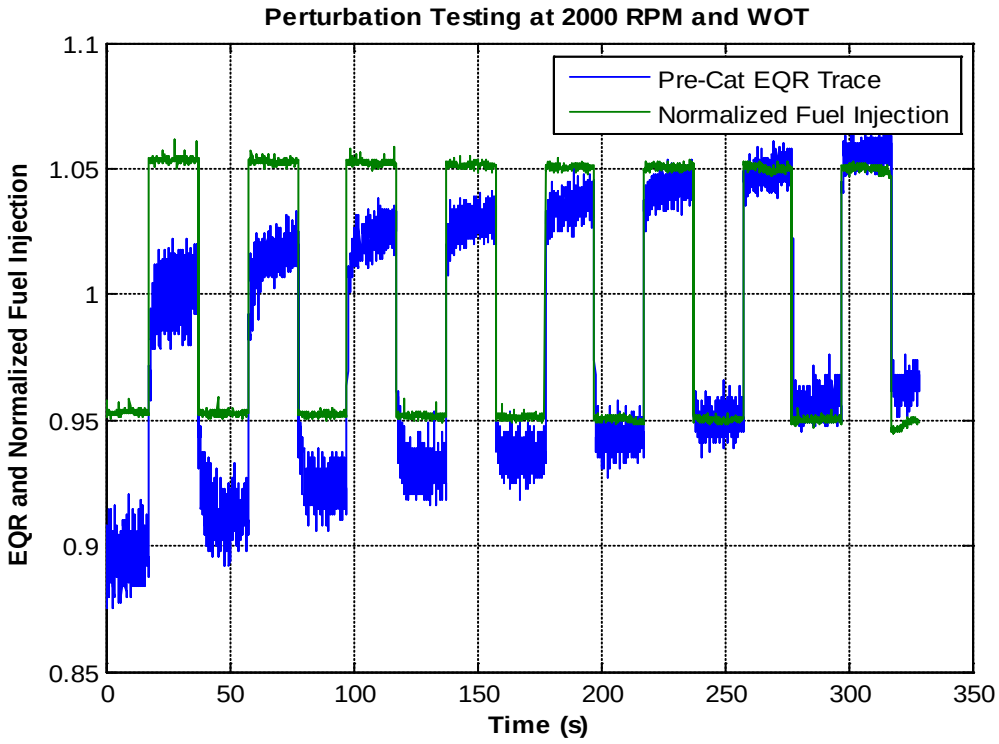

Figure 4:8: 2000 RPM and WOT Results

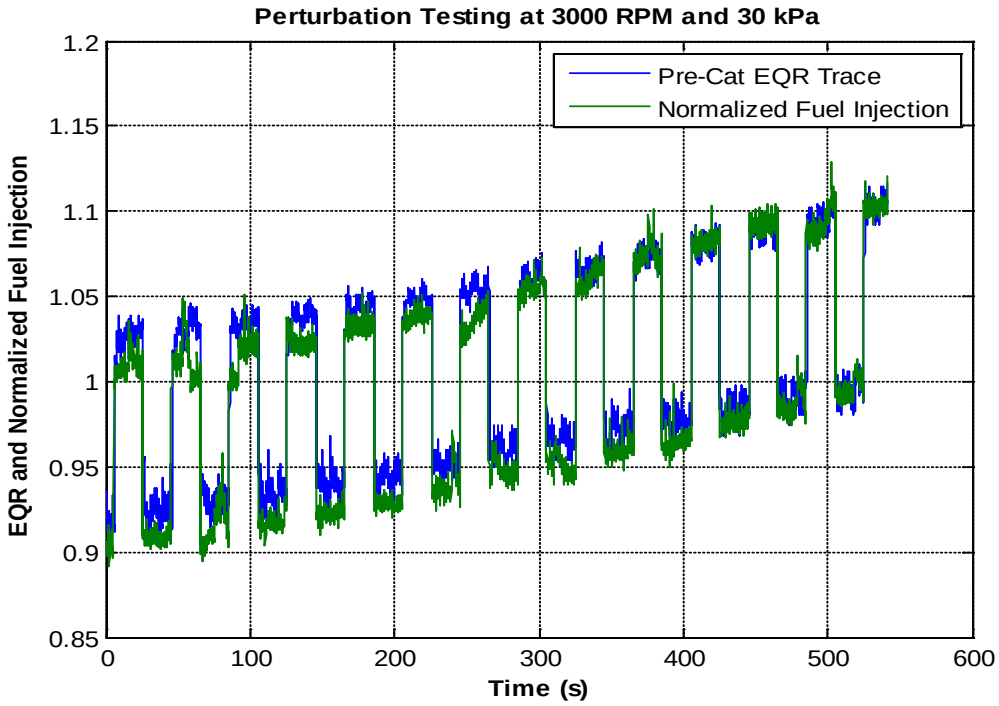

Figure 4:9: 3000 RPM and 30kPa Results

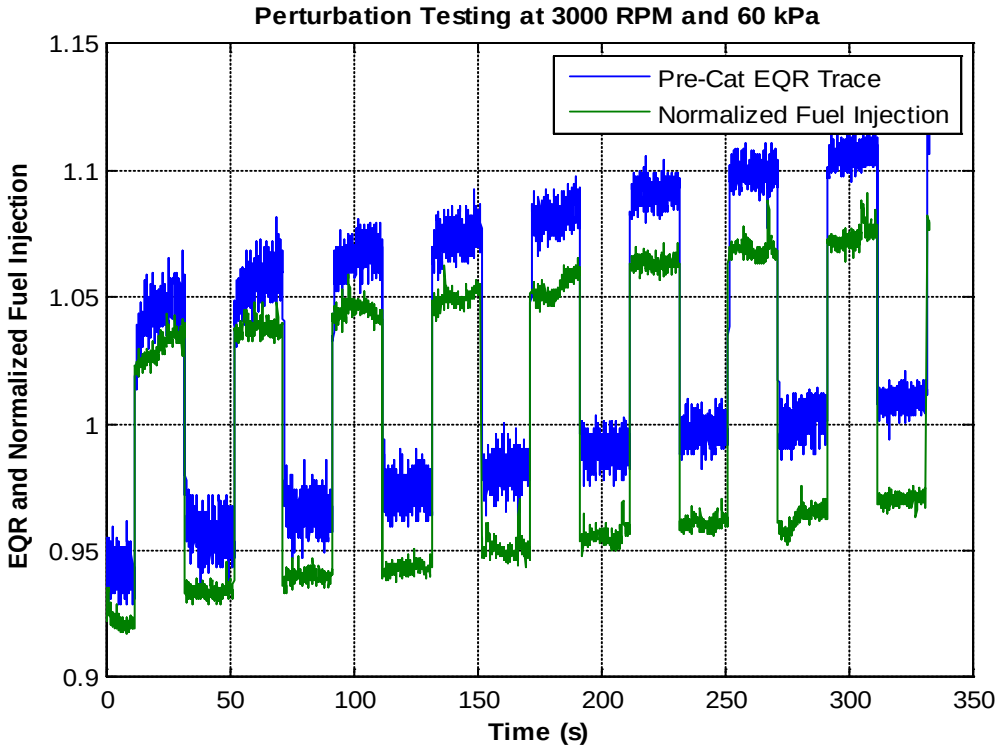

Figure 4:10: 3000 RPM and 60kPa Results

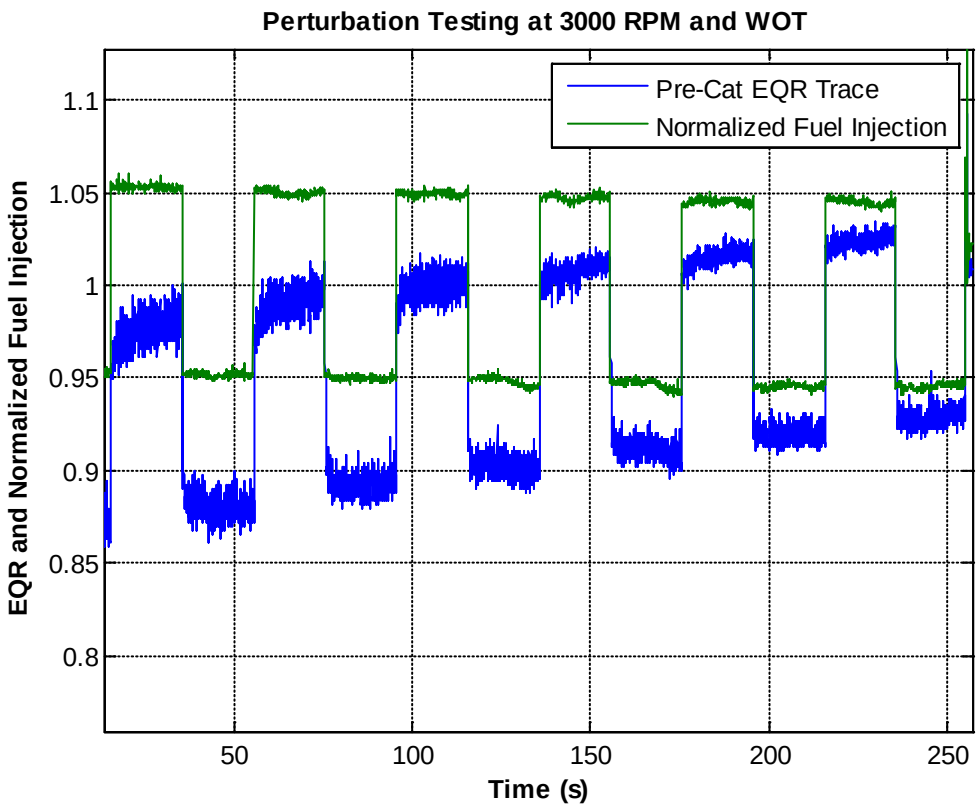

Figure 4:11: 3000 RPM and WOT Results

Chapter 5: τ AND X DETERMINATION

5.1 Experiment Results

In order to determine τ and X from collected data, the effects from the flow path of the fuel injected to the exhaust must be considered. Figure 5:1 below demonstrates this flow path and parameters in addition to τ and X that relate the fuel rate injected to the EQR. These parameters are the initial mass of the fuel puddle (m_p) and the total transport time delay(t_d).

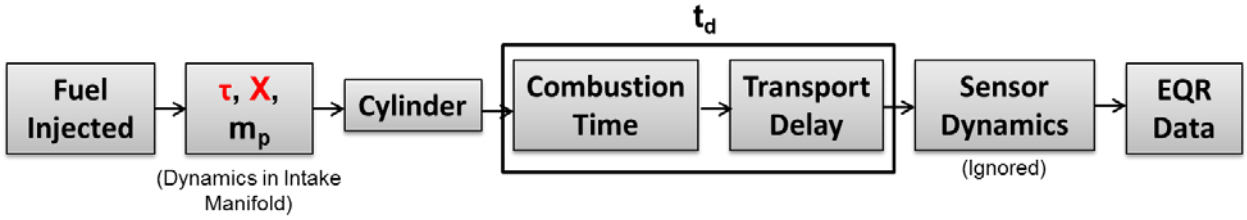

Figure 5:12: Flow of Fuel and Exhaust

5.2 Modeling Technique

Methods to determine τ and X often involve a model with the parameters that describe the fuel and exhaust flow. One method creates a fuel dynamics model that sends the fuel rate injected and guessed parameter values as inputs. The model modifies the parameters to achieve a best fit with calculated cylinder fuel rate from the EQR and mass air flow (MAF). The equation to determine the calculated cylinder fuel rate is shown in Equation 5.1 below. The data returned from this modeling technique is not always accurate because the additional parameters make fitting difficult.

$$\dot{m_{cyl}} = MAF * \frac{EQR}{9.87} \tag{5.1}$$

Part of the methods used in this research involves a similar modeling technique. This modeling method tries to approximate τ and X with greater accuracy by eliminating the m_p and t_d parameters. The t_d parameter is eliminated by using a MATLAB script with the ginput function to "cut out" each perturbation to be sent into the model. Cutting out the perturbation allows the user to pick the start and endpoint of the EQR trace perturbation and match it with the corresponding data point in the fuel rate injected. The calculated fuel rate entering the engine differs from the fuel rate recorded. This is because the ECU returns the commanded injected fuel rate, but the actual fuel rate injected is slightly different. Also, not all of the fuel is burned in combustion or reaches the exhaust sensor. This error is eliminated by normalizing the EQR trace from 0 to 1. The normalized trace is used to determine a theoretical step fuel input of 1 for an up perturbation or 0 for a down perturbation. Finally, a "normalized" initial mass puddle is determined by solving Equation 2.12 for the puddle mass with the first normalized EQR and fuel rate injected values. Equation 5.2 shows the calculation for the puddle mass.

$$m_p = \tau[\dot{m_{cyl}} - (1 - X)\dot{m_{inj}}] \tag{5.2}$$

The modeling technique used differs from others in the way it estimates τ and X. Instead of approximating τ and X by fitting the calculated cylinder fuel rate with an approximate cylinder fuel rate, the technique varies τ and X so that the sum of the error between the calculated cylinder fuel rate and the approximate is a minimum. The function used to find this minimum error is the fminsearch function in MATLAB. A pictorial representation of this method is shown in Figure 5:2 below.

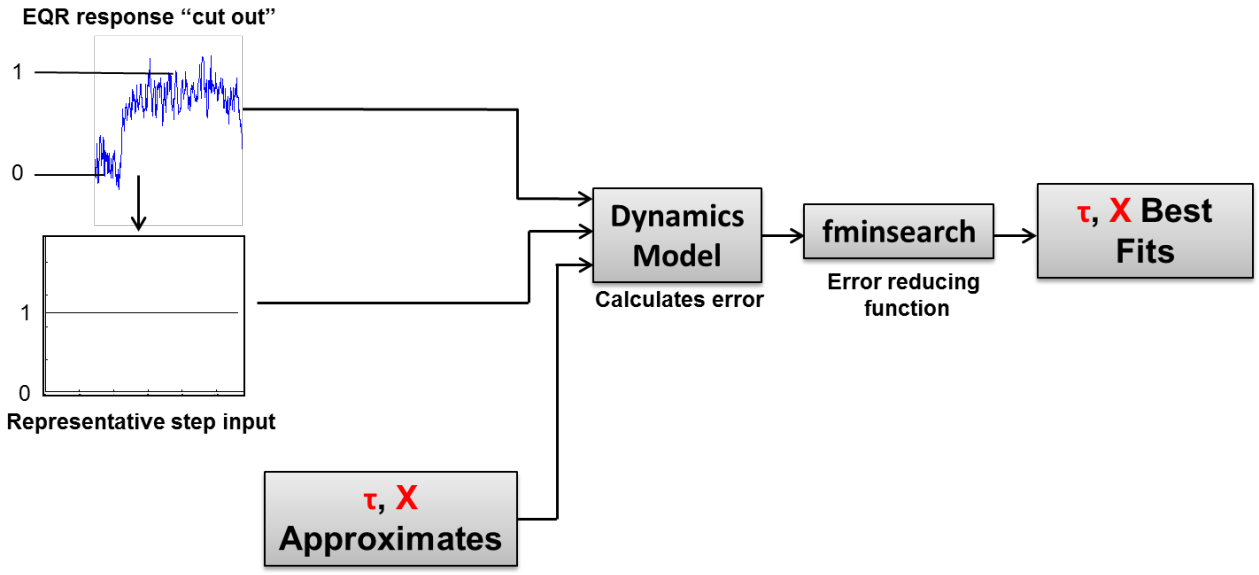

Figure 5:13: Modeling Technique Representation

5.3 Initial Method

An initial MATLAB script file was created for each of the nine perturbation experiments utilizing the modeling technique described above. Sample code for the 2000 RPM and 60kPa experiment is located in Appendix C.

Two Simulink models describing the fuel dynamics were run by the script file. The models were developed to solve the fuel dynamics equations more easily instead of using MATLAB code. The first Simulink model was run through the fminsearch function to return an error value. This model and its subsystems are shown as Figures 9:4 through 9:6 in Appendix D. The second Simulink model was nearly identical to the first except its output returned the calculated cylinder fuel rate with τ and X to compare with the experimental cylinder fuel rate and the theoretical step input. This model is shown in Appendix D as Figure 9:7.

5.4 Initial τ and X Results

The previously described methods were used to determine the τ and X results for each of the nine perturbation experiments. Figure 5:3 shows a sample of τ data for the 2000 RPM and 60 kPa case. The arrows show data outliers from the expected results. The remaining points appear to follow similar to expected results. Figure 5:4 shows a sample of X data for the 2000 RPM and 60 kPa case. The X data has no discernible trends. Similar trends occurred for the other engine speed and MAP cases as well. A new methodology was needed to better approximate X values.

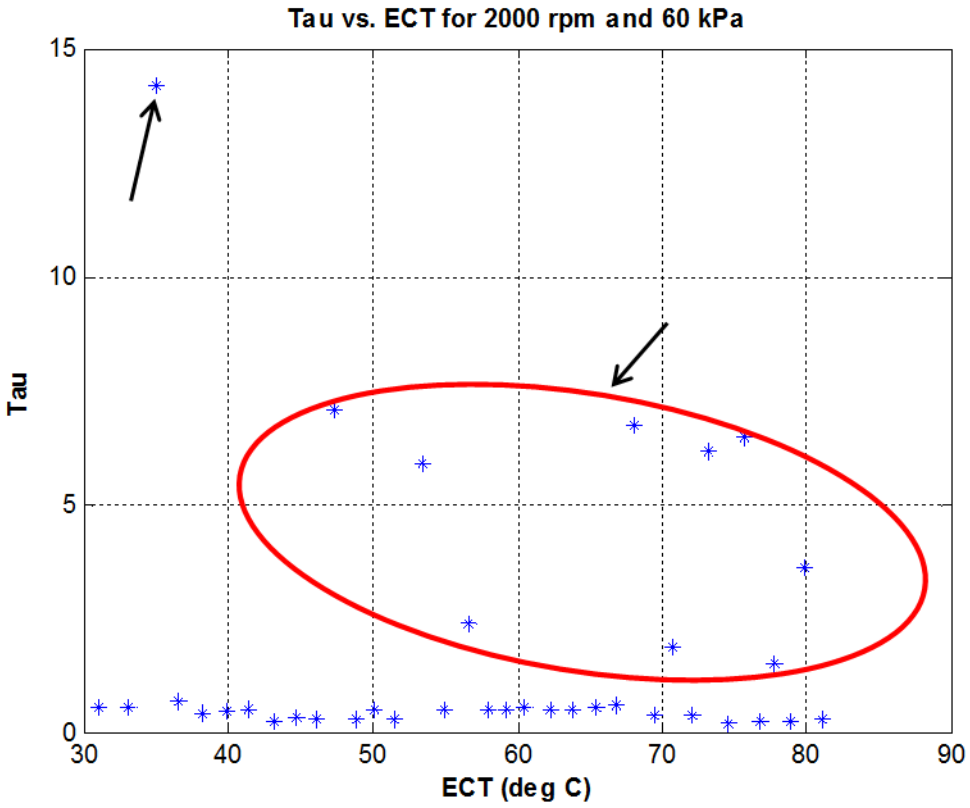

Figure 5:14: Sample τ vs. ECT Data for 2000 RPM and 60kPa with Outliers

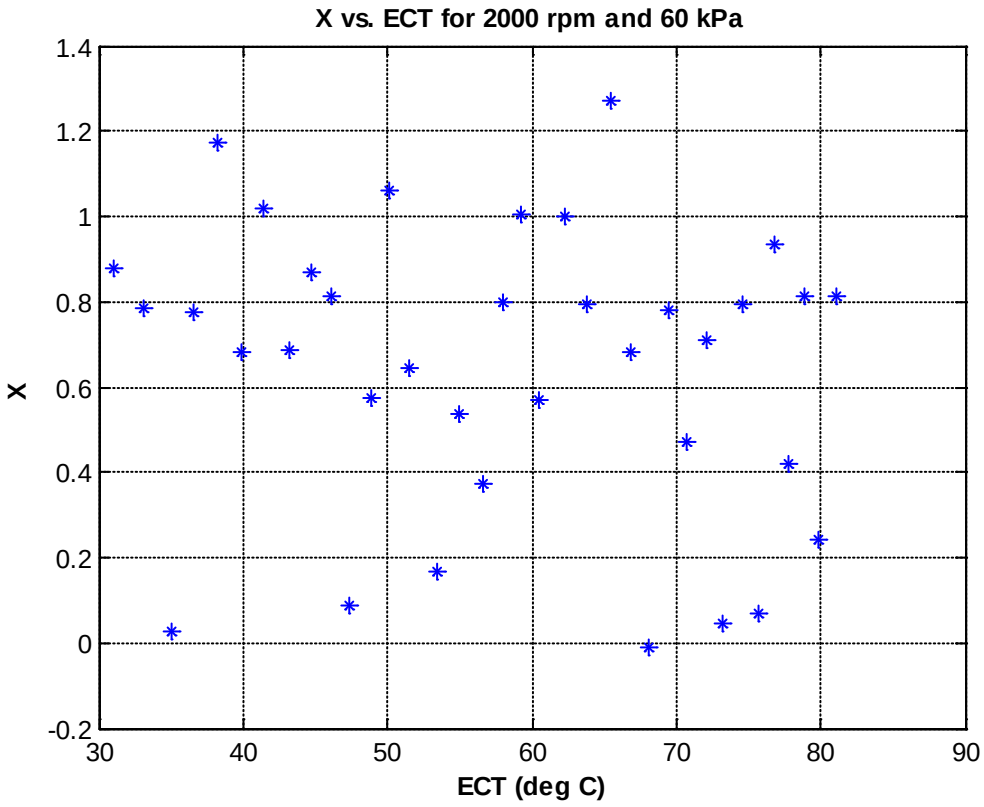

Figure 5:15: Sample X vs. ECT Data for 2000 RPM and 60 kPa

5.5 Initial Methodology Issues

After observing the initial results, the primary issues with the first method were reviewed. First, the code evaluated error over the entire EQR response where τ and X no longer had an effect on the response. Second, the fminsearch function picked unreasonable τ and X values which would cause the calculated fuel rate to diverge, and the code would stop functioning. Finally, the code was returning some expected τ value trends but not X values.

5.6 Second Method

The second method used to determine the τ and X parameters addressed the initial methodology issues. This method normalizes adjacent up and down perturbation cut outs and

repeats them over several cycles with a repeated sequence block on Simulink. The initial dynamics model was updated with logic to limit error evaluation only where τ and X affect the response. This was accomplished by evaluating error when the calculated response was between 0.05 and 0.95. The model also has logic to reinitialize error evaluation over the entire experimental response if the calculated response escapes values above 2 or below -1. This prevents the possibility of a diverging calculated response. The fmincon function was used to constrain the τ and X parameters within reasonable values to also prevent diverging responses. Figure 5:5 shows a pictorial representation of the methodology. A second method code sample is presented in Appendix C, and the updated Simulink model is shown in Appendix D as Figure 9:8.

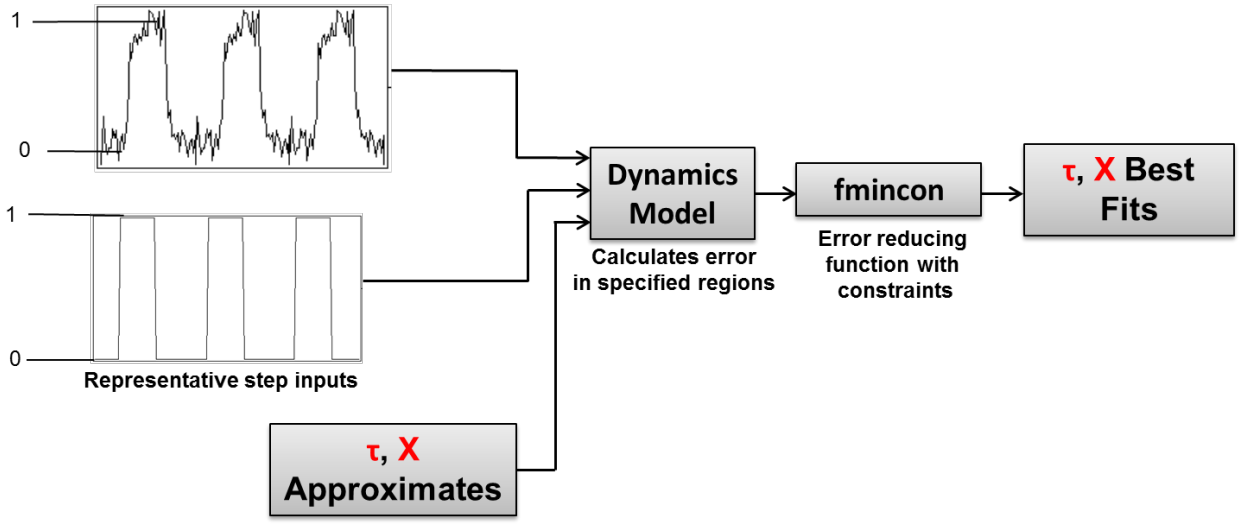

Figure 5:16: Representation of Second Methodology

5.7 Second Method Results

Figures 5:6 and 5:7 show calculated τ values for selected cases. The number of data points returned was halved from the first method because a set of up and down perturbations was needed to calculate each data point. The results show that τ follows anticipated trends. The

outlying data points in τ values were usually close to values of 6. This is likely caused from the initial guess in fmincon of 6. If fmincon was unable to reduce error, the function returned its initial input value.

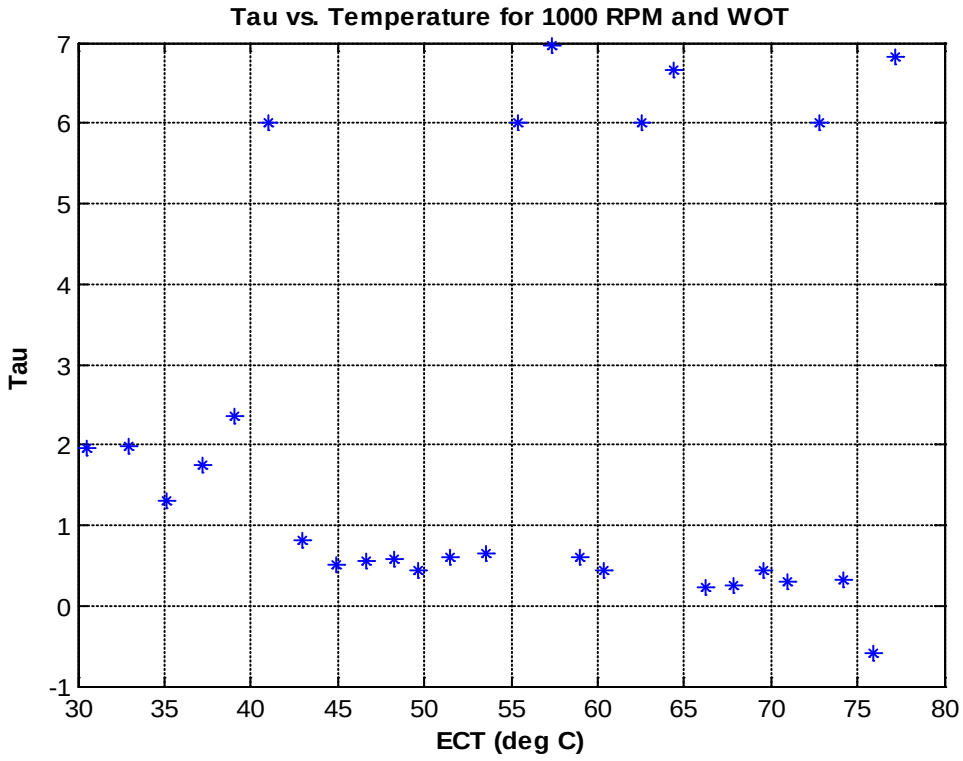

Figure 5:17: Current τ vs. ECT Data for 1000 RPM and WOT Case

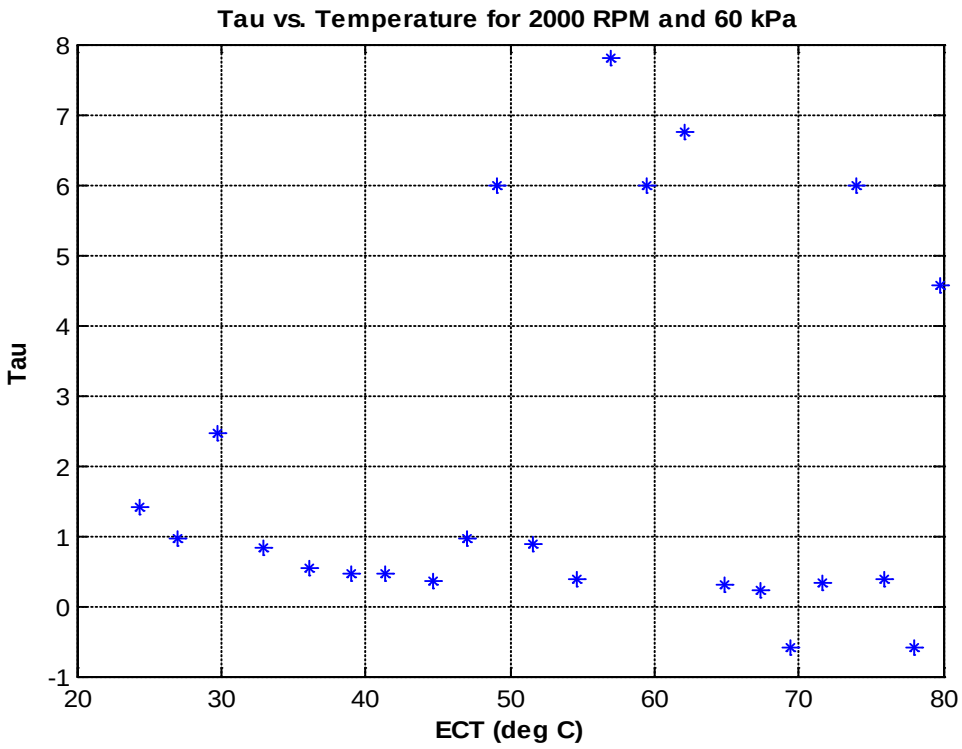

Figure 5:18: Current τ vs. ECT Data for 2000 RPM and 60 kPa Case

Because the τ data excluding outliers followed anticipated trends, curve fits were determined for each of the nine engine speed and manifold air pressure cases. Two-term power curve fits were made using a MATLAB curve fit tool (cftool). Power curve fits were used because they displayed the best coefficient of determination values for τ. Figure 5:8 below shows an example τ curve fit with cftool. Table 5:1 shows the coefficient of determination values for each τ case. Figures 5:9 through 5:11 display τ curve fits for set MAP and varying RPM.

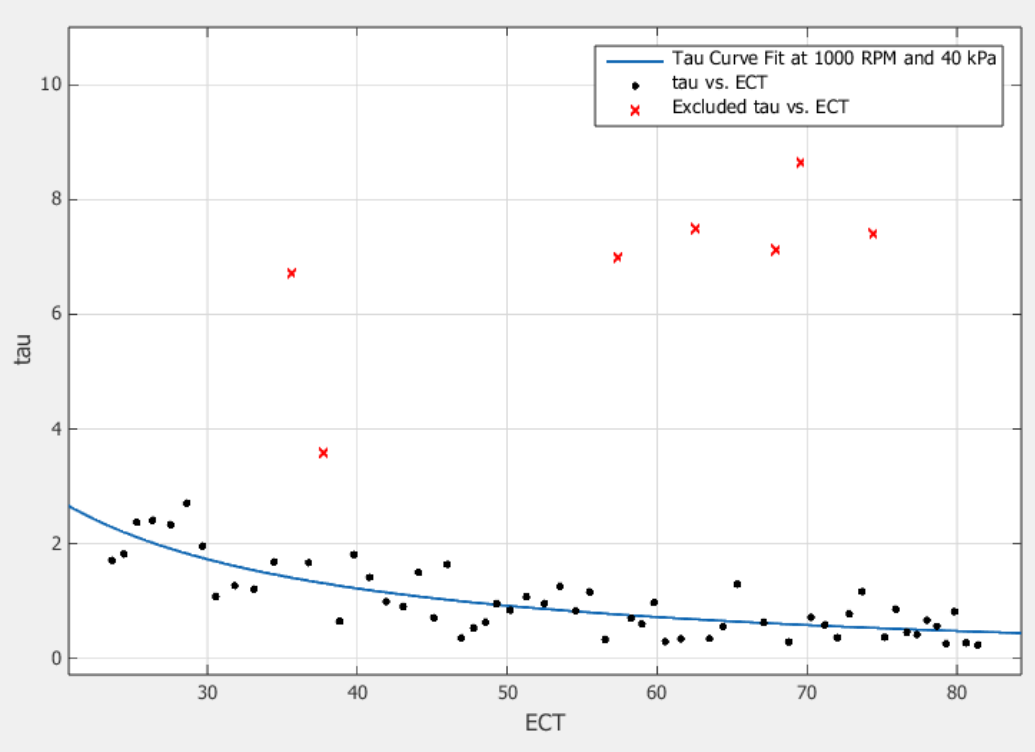

Figure 5:19 Two-Term Power Curve Fit for τ vs. ECT

Table 5:1: Coefficient of Determination Values for τ

τ Coefficient of Determination	30 or 40 kPa	60 kPa	WOT
1000 RPM	0.6885	0.9220	0.7608
2000 RPM	0.7759	0.4655	0.2021
3000 RPM	0.9124	0.8866	0.9800

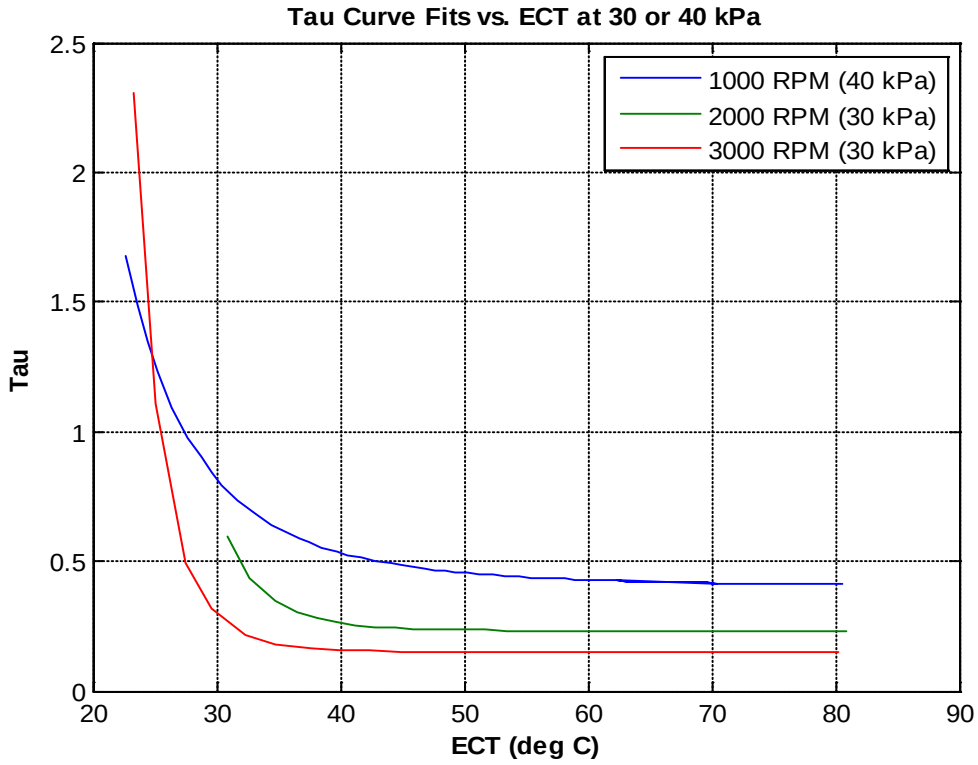

Figure 5:20: τ Curve Fits at 30 or 40 kPa

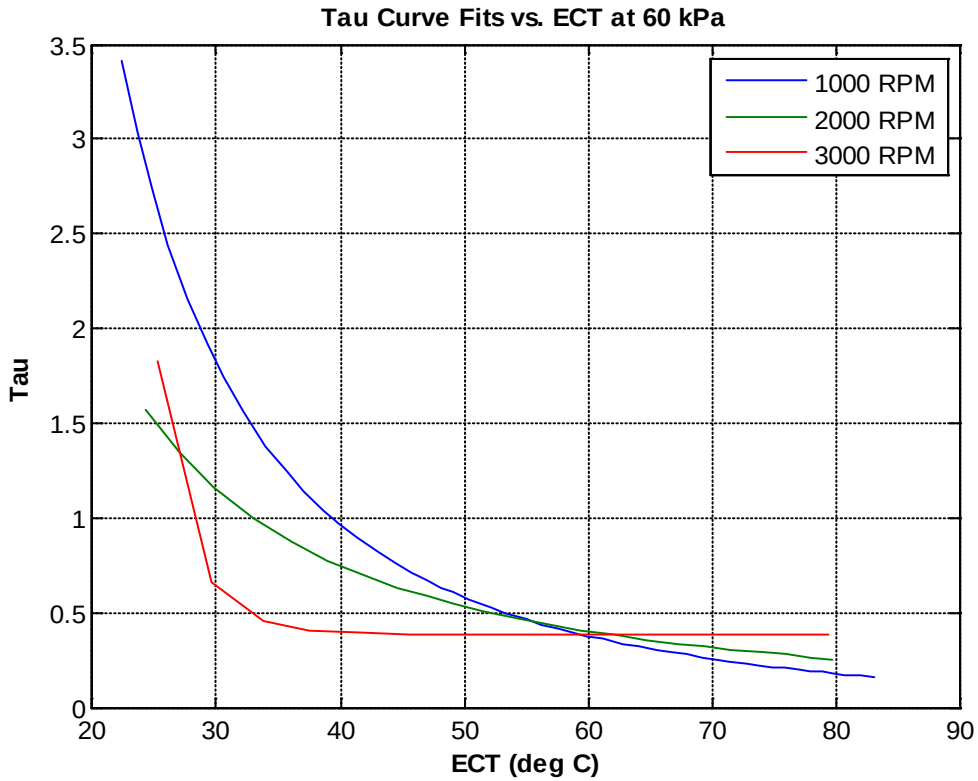

Figure 5:21: τ Curve Fits at 60 kPa

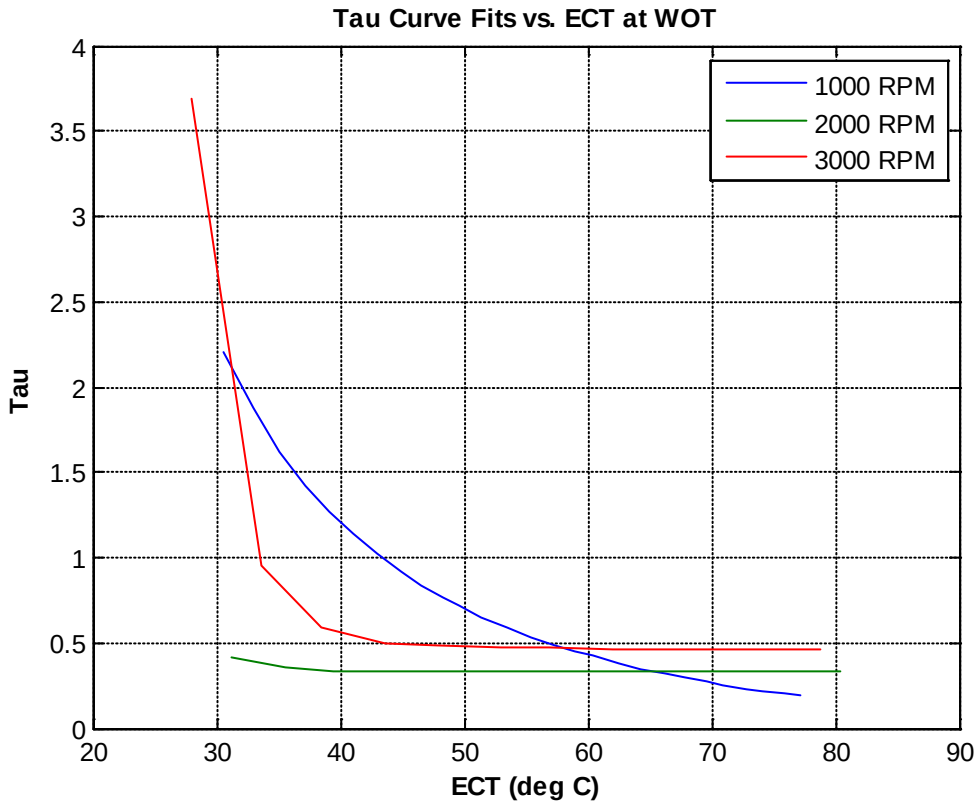

Figure 5:22: τ Curve Fits at WOT

Figures 5:12 and 5:13 display the sample X values for two cases. The X values again show little to no expected trends. The two primary causes of improper X values were determined to come from the method used to calculate X and from noisy data. Because the X effects on the fuel response are smaller relative to the τ effects, the returned X values did not need to be accurate to produce little error. Also, the noisy data made determining the 1-X "jump" difficult to locate. Figure 5:14 shows how noisy data can yield multiple values for 1-X and therefore X.

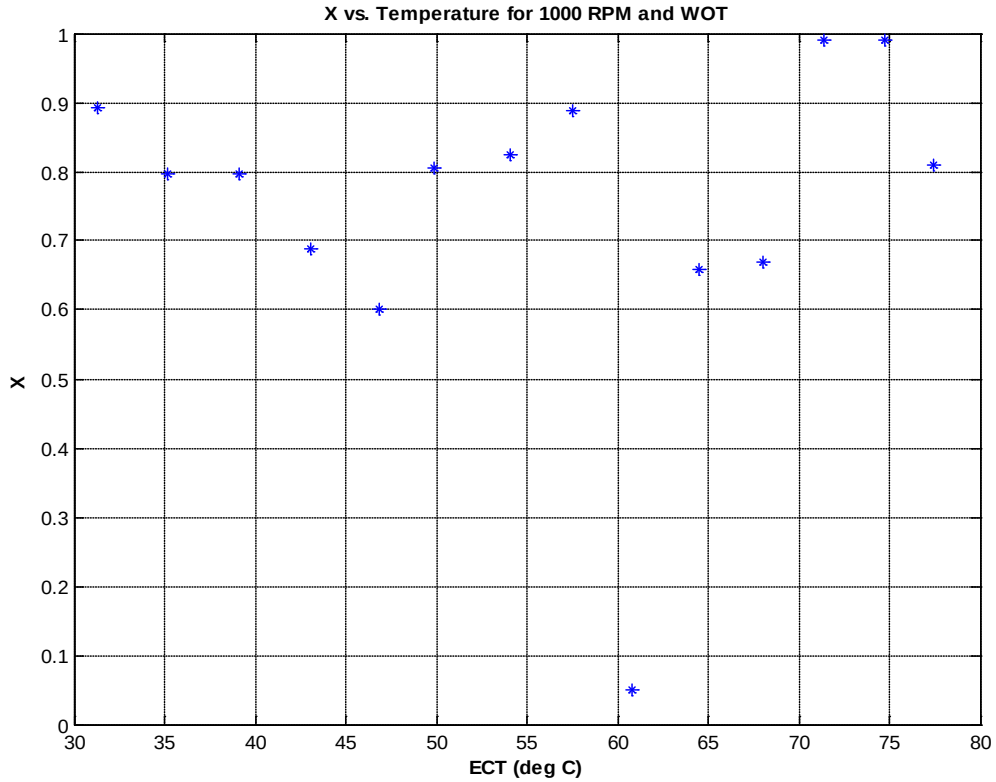

Figure 5:23: Second Method X vs. ECT Data for 1000 RPM and WOT Case

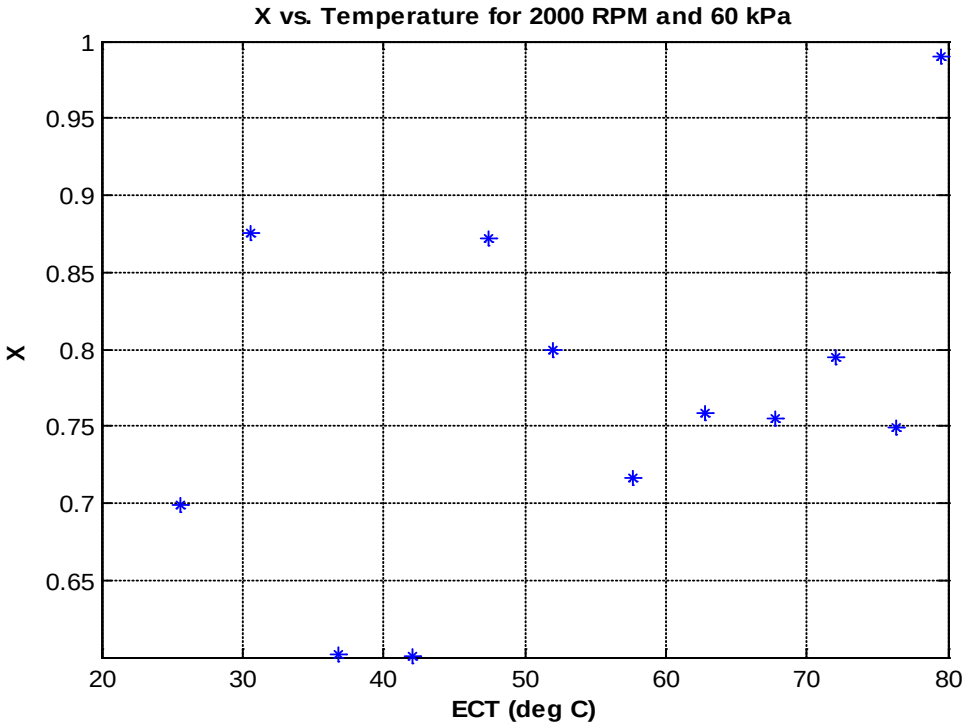

Figure 5:24: Second Method X vs. ECT Data for 2000 RPM and 60 kPa Case

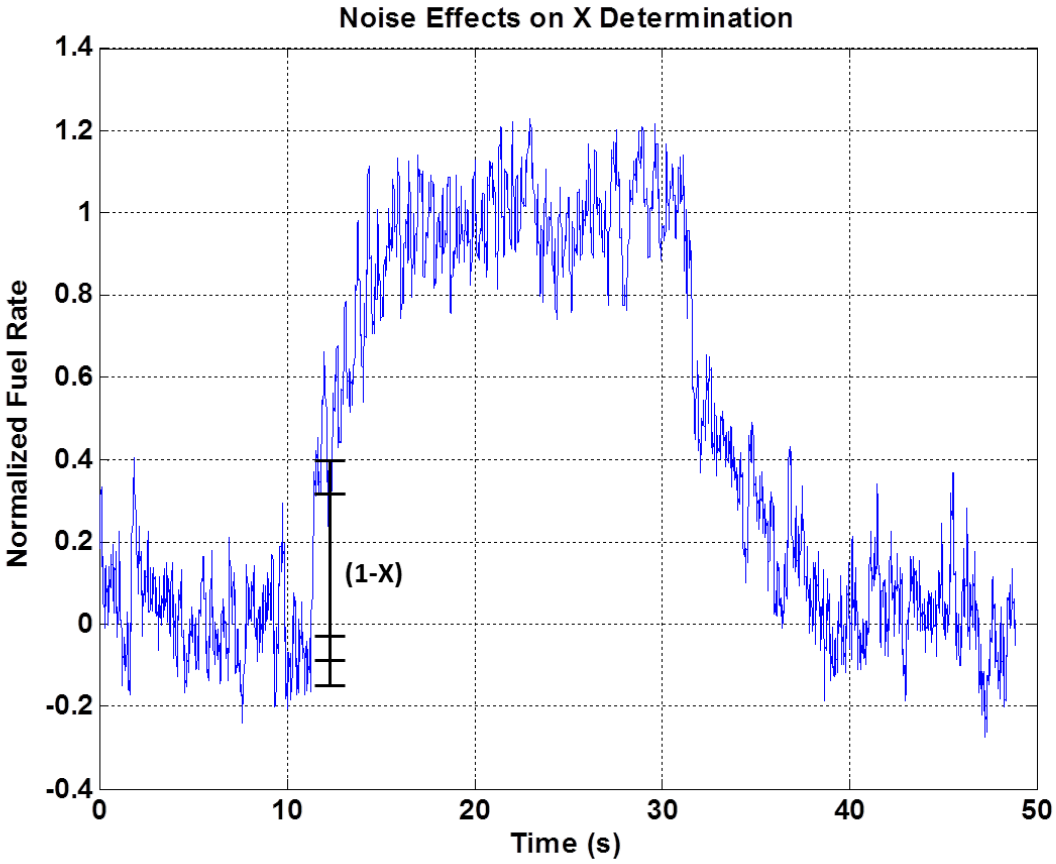

Figure 5:25: Noise Effects on X Determination

5.8 X Determination Method

Because the X values continued to show more scatter than returned τ values, an X determination method was implemented to return results closer to expected trends. This method involved calculating each X value for the nine cases by inspection of the normalized fuel rate. The 1-X value can be calculated from a normalized EQR response because X is unitless. The magnitude of the response is 1, so finding the change in normalized fuel rate of the fuel "jump" is equivalent to 1-X. Each X value was calculated by hand from the normalized EQR response.

5.9 X Results

Figures 5:15 and 5:16 demonstrate sample X values calculated from the inspection method. The X values are similar to the values for E85 fuel in Section 2.3.2.2. The calculated data was accurate enough to make linear curve fits without excluding outliers. Table 5.3 shows the coefficient of determination values for each X case. Figures 5:17 through 5:19 display X curve fits for constant MAP and varying RPM.

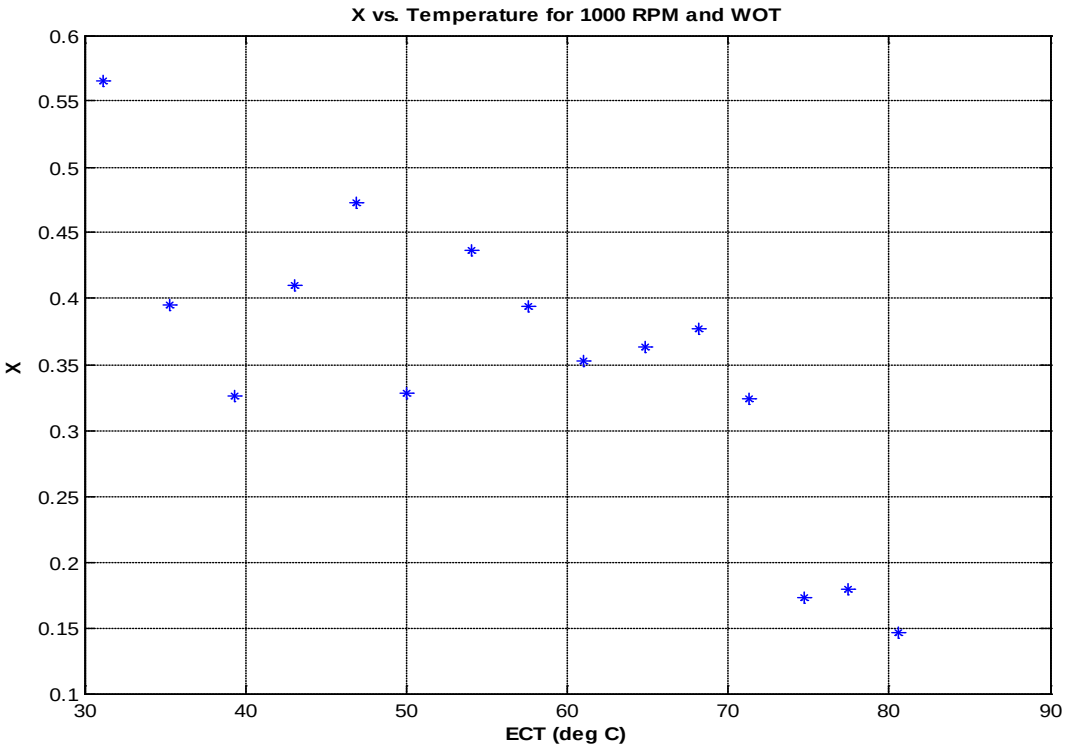

Figure 5:26: X Values from Inspection at 1000 RPM and WOT

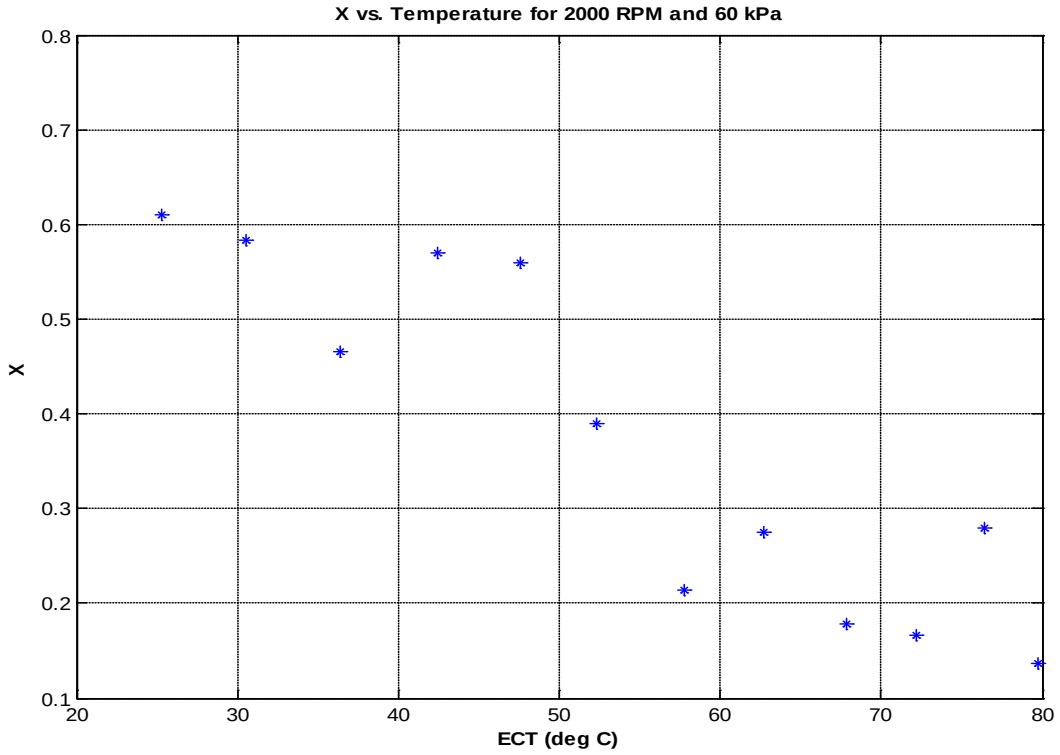

Figure 5:27: X Values from Inspection at 2000 RPM and 60 kPa

Table 5:2: Coefficient of Determination Values for X

X Coefficient of Determination	30 or 40 kPa	60 kPa	WOT
1000 RPM	0.4213	0.8839	0.6098
2000 RPM	0.3292	0.8223	0.555
3000 RPM	0.7217	0.6299	0.2384

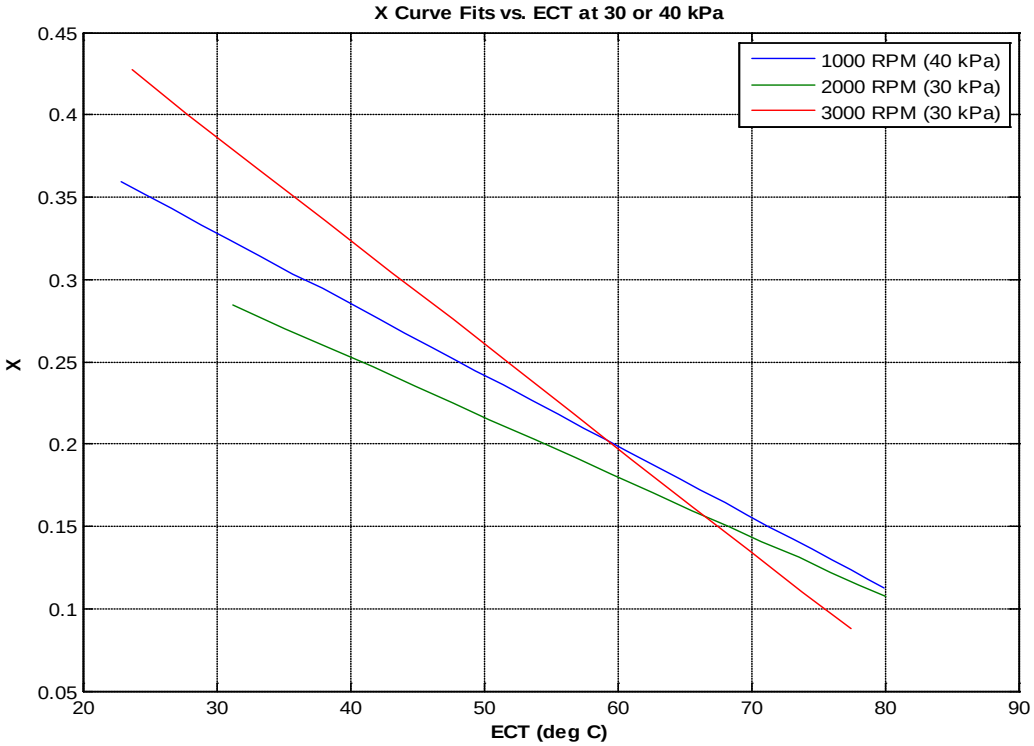

Figure 5:28: X Curve Fits at 30 or 40 kPa

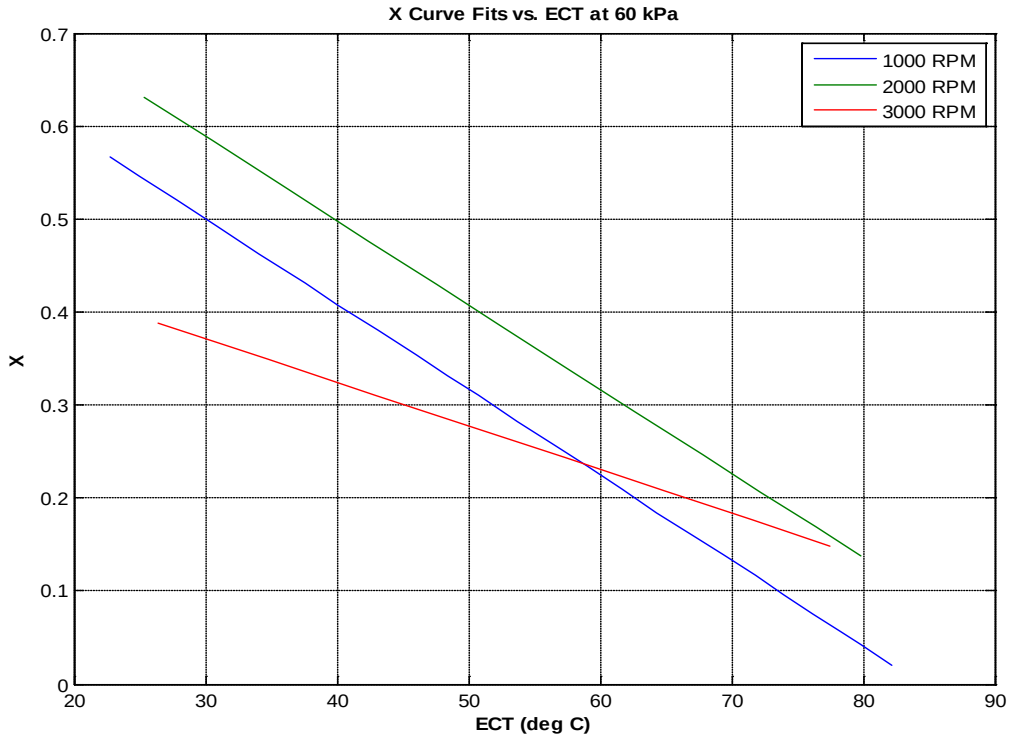

Figure 5:29: X Curve Fits at 60 kPa

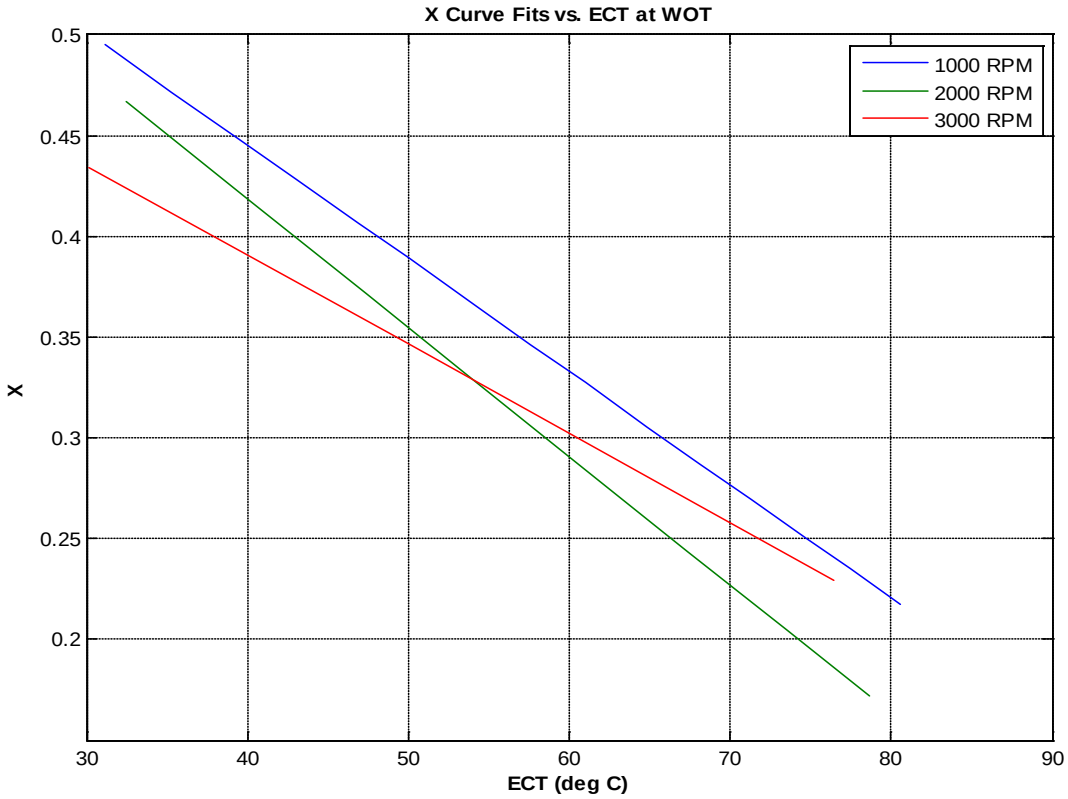

Figure 5:30: X Curve Fits at WOT

Although the X curve fits generally follow the expected trends, several deviations are noticeable. The fits deviate from the expected results for the 2000 RPM and 60 kPa case and the 1000 RPM and 40 kPa case. The X values should also get larger with increasing MAP but do not from 60 kPa to WOT in the 2000 and 3000 RPM cases. The deviations seen in these fits are likely the result of improper X calculation from noisy data as well as human error from hand calculations. In addition, the lower number of data points for higher engine speeds and MAPs make accurate curve fitting for these operating conditions less likely.

Chapter 6: VALIDATION AND IMPLEMENTATION OF FUEL COMPENSATOR

6.1 Introduction

In order for the calculated τ and X parameters to have an effect on reducing emissions, they must be implemented into the vehicle control software. The current fuel dynamics algorithm in the Honda engine controller is not being used because the current τ and X parameters are not correct.

The method for developing a fuel compensator algorithm is to use the fuel dynamics equation to solve for the fuel rate injected as shown in Equation 6.1. The cylinder fuel flow rate becomes the desired fuel rate, and the τ and X parameters are known. The puddle mass at start-up is 0; however, the puddle mass must be known at every ECU time increment to properly compensate the fueling. The puddle mass can be calculated by integrating the difference between the compensated fuel rate and the desired fuel rate. Once a fuel compensator algorithm is created, it can be implemented into the ECU to correct the injected fuel rate for fuel dynamics as the engine warms.

$$\dot{m}_{inj} = \frac{1}{1-X}\left(\dot{m}_{des} - \frac{1}{\tau} m_p\right) \tag{6.1}$$

6.2 τ and X Implementation

When creating the algorithm for the engine control code, several precautions were taken with the τ and X data. Because the data deviates from the expected trends in some cases, the algorithm will not function at its optimal capabilities at these operating conditions. More data collection is desired at engine operating conditions where the data trends deviate from expected. Because the X data showed similar results through all nine cases, a representative X curve fit

shown in Figure 6:3 was determined from all collected X data points for the compensator. Three τ curve fits were also created for each engine speed because the data was similar for different MAP cases. The new X and τ curve fits created in cftool are displayed in Appendix E as Figures 9:10 through 9:13.

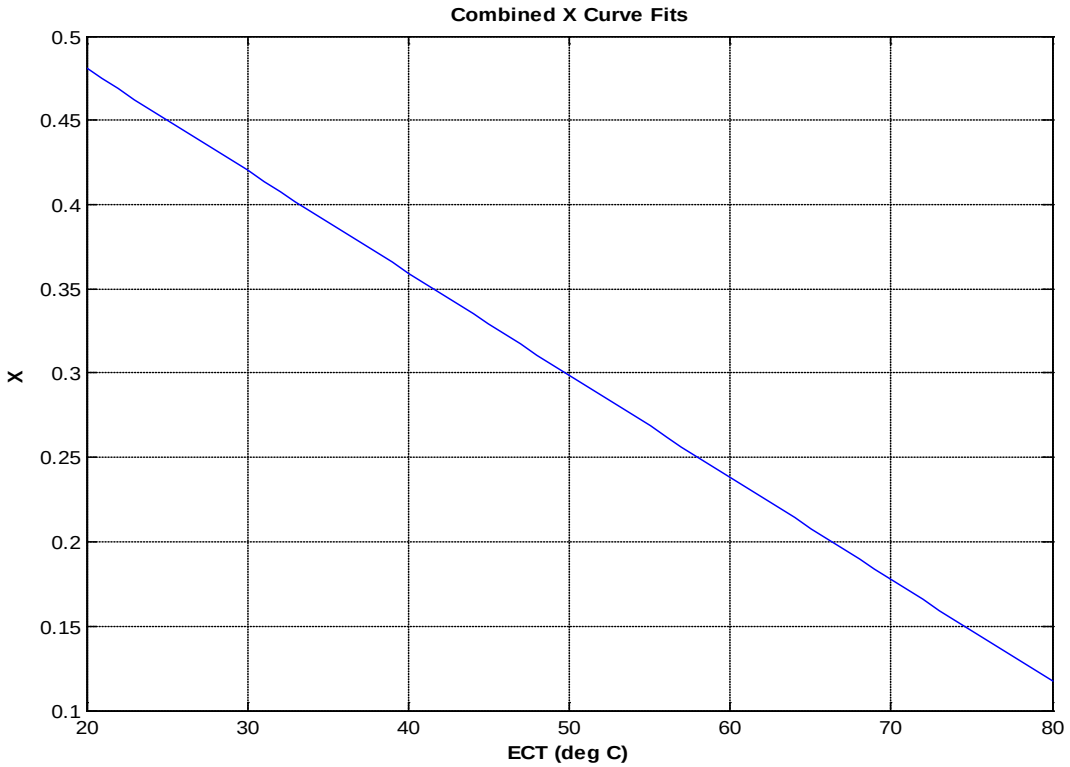

Figure 6:31: Averaged X Curve Fit for All Data Points

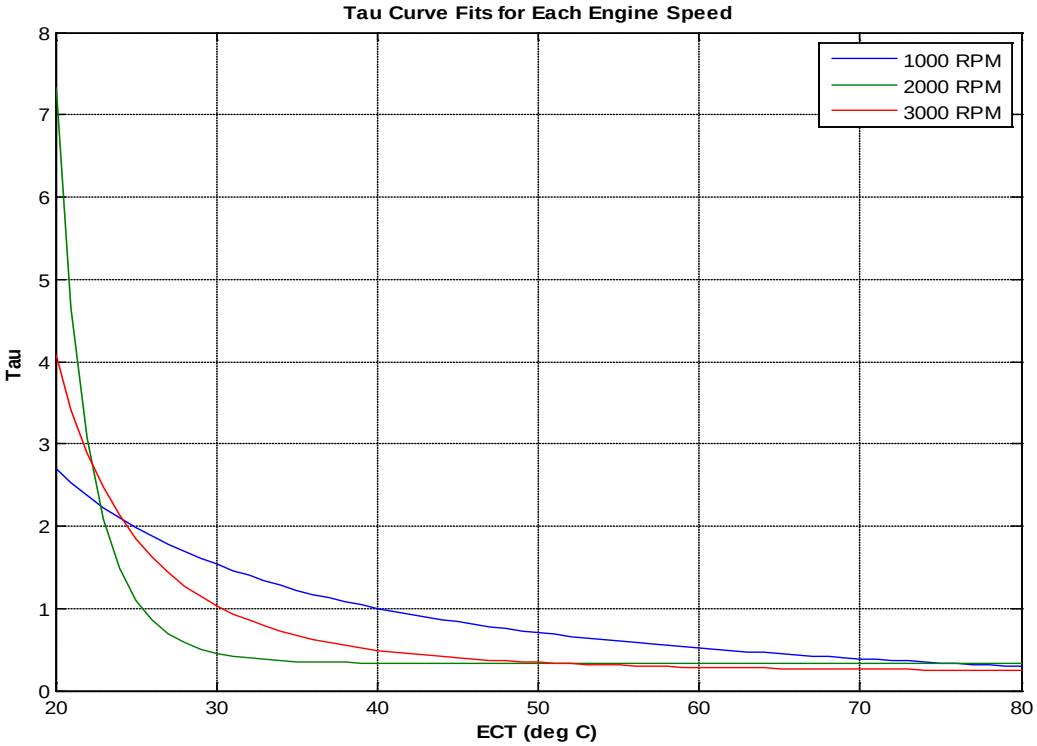

Figure 6:32: Averaged τ Curve Fits for Engine Speeds and ECT

6.2.1 Lookup Tables

To ensure a fast and accurate fuel compensator algorithm, it is desired to calculate τ and X as functions of engine operating characteristics simultaneously. In Simulink and control development, lookup tables are used for these purposes. Lookup tables receive an input or multiple input values and output interpolated values based off of previously stored data. The X fit curve and three τ fit curves in Figures 6:1 and 6:2 were implemented into lookup tables in the algorithm to determine τ and X values at different operating conditions.

The output data of the lookup tables were saturated within the reasonable values. Without saturation, input values beyond the ranges seen in the perturbation experiments may result in incorrect τ and X values. For example, some engine temperatures exceeding 80° C will yield X values less than 0. The X output values are saturated within 0.05 to 0.6. The output τ values were

saturated within 0 to 4. Figure 6:3 shows an illustration of the τ and X lookup tables created in Simulink for the compensator algorithm.

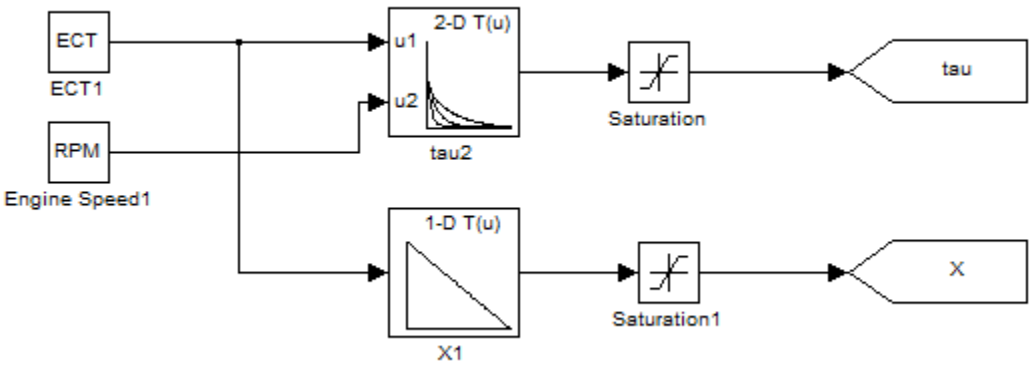

Figure 6:33: Simulink Lookup Tables

6.3 Fuel Compensator Validation

A fuel compensator algorithm as described previously was created in Simulink. The Simulink model is located in Appendix D as Figure 9:9. To validate that the compensator works correctly, square wave desired fuel injection rates were sent into the model, and the compensated output fuel rate was returned. In order to compensate fuel dynamics, the compensated fuel injected overshoots or undershoots the fuel at the start of each perturbation to obtain the desired square wave fuel rate at the engine cylinder. Figure 6:2 demonstrates that the algorithm correctly compensates the fuel rate as described previously. The model's effectiveness depends on how accurate the τ and X parameters in the algorithm's lookup tables are.

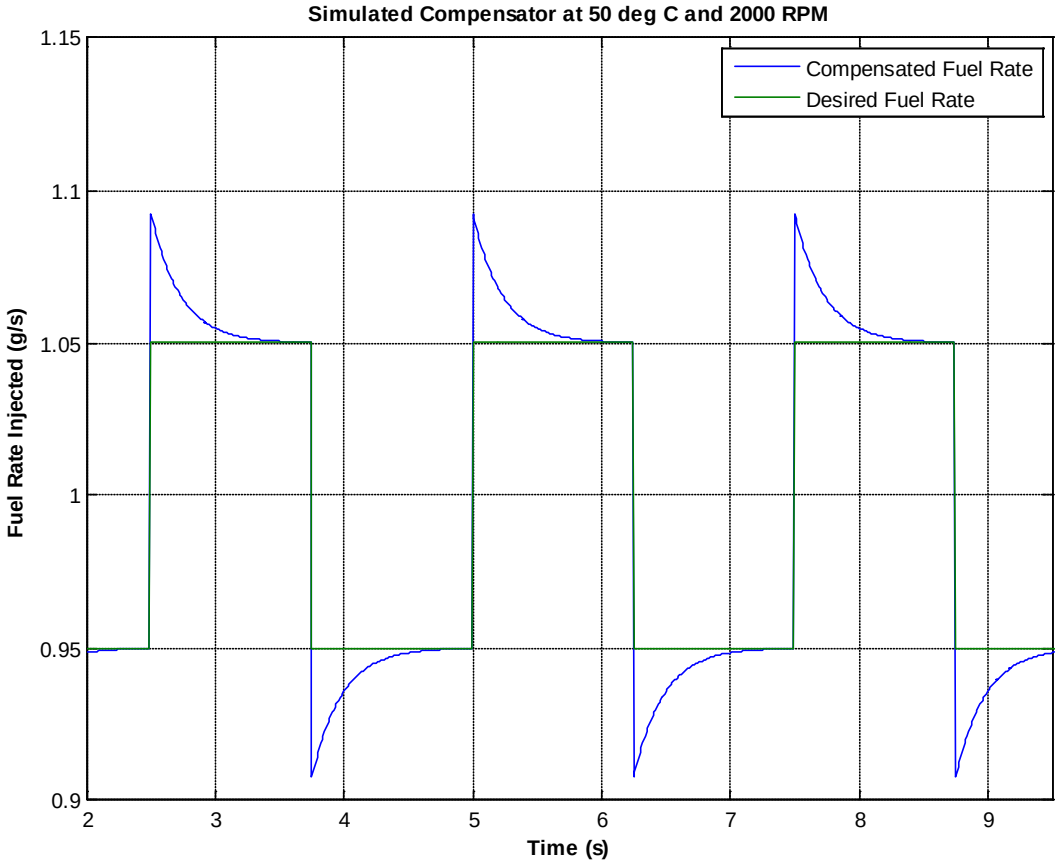

Figure 6:34: Simulated Desired and Compensated Fuel Rates

6.4 Emission Reduction Validation

Once the algorithm has been implemented into the engine control code, further tests can be performed to determine the algorithm's effectiveness during cold starts. The tests would occur at different operating conditions with the compensator algorithm enabled and disabled. A Horiba exhaust gas analyzer can be used to determine the difference in emissions with or without the compensator during cold starts.

Chapter 7: CONCLUSIONS AND FUTURE WORK

This research successfully demonstrates methods to reduce cold start emissions from transient fuel dynamics. A model of the fuel dynamics was used several times to determine the τ and X parameters. Several different methods were utilized to determine the most accurate results. More data points, especially at high engine speeds and MAPs, are needed to verify expected trends. Current τ and X data is lumped into four total fit curves to ensure anticipated trends with more data points. A working fuel compensator algorithm has successfully been completed and can be implemented into the engine code for use or for testing purposes.

Several forms of future work are planned. First, more testing is desired for more accurate τ and X data for the various operating conditions. A more accurate compensator will have two 3-D lookup tables for τ and X as functions of engine speed, MAP, and temperature. Second, heated fuel injectors will be implemented onto the Honda engine, and the process for creating a transient fuel compensator will be repeated for HFIs. The goal is to determine if the heated fuel injectors will require different fuel compensation parameters from the regular fuel injectors. Finally, an analysis on the emissions reduction after the fuel compensator has been implemented is desired.

My future plans are to attend Ohio State this upcoming school year and pursue a Master's Degree in Mechanical Engineering. I intend to continue automotive related research particularly in powertrain related topics.

Chapter 8: BIBLIOGRAPHY

[1] U.S. Environmental Protection Agency, (n.d.). *Six Principal Pollutants*. Retrieved from website: http://www.epa.gov/airtrends/2007/report/sixprincipalpollutants.pdf

[2] Yanowitz, J., & McCormick, R. U.S. Department of Energy, (2009). *Effect of E85 on Tailpipe Emissions from Light-Duty Vehicles*. Retrieved from website: http://www.afdc.energy.gov/pdfs/technical_paper_feb09.pdf

[3] Karpuk, M. U.S. Environmental Protection Agency, (n.d.). *Catalysts for the Control of Automotive Cold Start Emissions*. Retrieved from website: http://cfpub.epa.gov/ncer_abstracts/INDEX.cfm/fuseaction/display.abstractDetail/abstract/1450

[4] U.S. Environmental Protection Agency, (2010). *Conversion Factors for Hydrocarbon Emission Components* (NR-002d). Retrieved from website: http://www.epa.gov/otaq/models/nonrdmdl/nonrdmdl2010/420r10015.pdf

[5] Heywood, J. B. (1988). *Internal Combustion Engine Fundamentals.* New York: McGraw-Hill.

[6] Heimrich, M., *Air Injection to an Electrically-Heated Catalyst for Reducing Cold-Start Benzene Emissions from Gasoline Vehicles*, SAE Paper No. 902115, 1990.

[7] Bezaire, B. A. (2011). *Modeling and Control of an Electrically-Heated Catalyst*. Columbus: Ohio State University, M.S. Thesis.

[8] Rizzoni, G. *ME 7226 Powertrain Dynamics: Module 3*

[9] Batteh, J., Curtis, E., and Fried, M., *Analytical Assessment of Simplified Transient Fuel Tests for Vehicle Transient Fuel Compensation*, SAE Paper No. 2005-01-3894, 2005.

[10] Hendricks, E., et all, *Nonlinear Transient Fuel Film Compensation (NTFC)*, SAE Paper No. 930767, 1993.

[11] Almkvist, G. and Eriksson, S., *A Study of Air to Fuel Transient Response and Compensation with Different Fuels*, SAE Paper No. 941931, 1994.

[12] Ahn, K., Stefanopoulou, A., and Jankovic, M., *Puddle Dynamics and Air-to-Fuel Ratio Compensation for Gasoline-Ethanol Blends in Flex-Fuel Engines*, SAE Paper No. 941931, 1994.

[13] Shayler, P.J. *Fuel Transport Characteristics of Spark Ignition Engines for Transient Fuel Compensation*, SAE Paper No. 950067, 1995.

[14] Kabasin, D., et all, *Heated Injectors for Ethanol Cold Starts*, SAE Paper No. 2009-01-0615, 2009.

[15] Everett, R. (2010). *Transient Air Dynamics Modeling for an Advanced Alternative Fueled Engine*. Columbus: The Ohio State University, Undergraduate Honors Thesis.

Chapter 9: APPENDIX

APPENDIX A: Simulink Engine Control Model

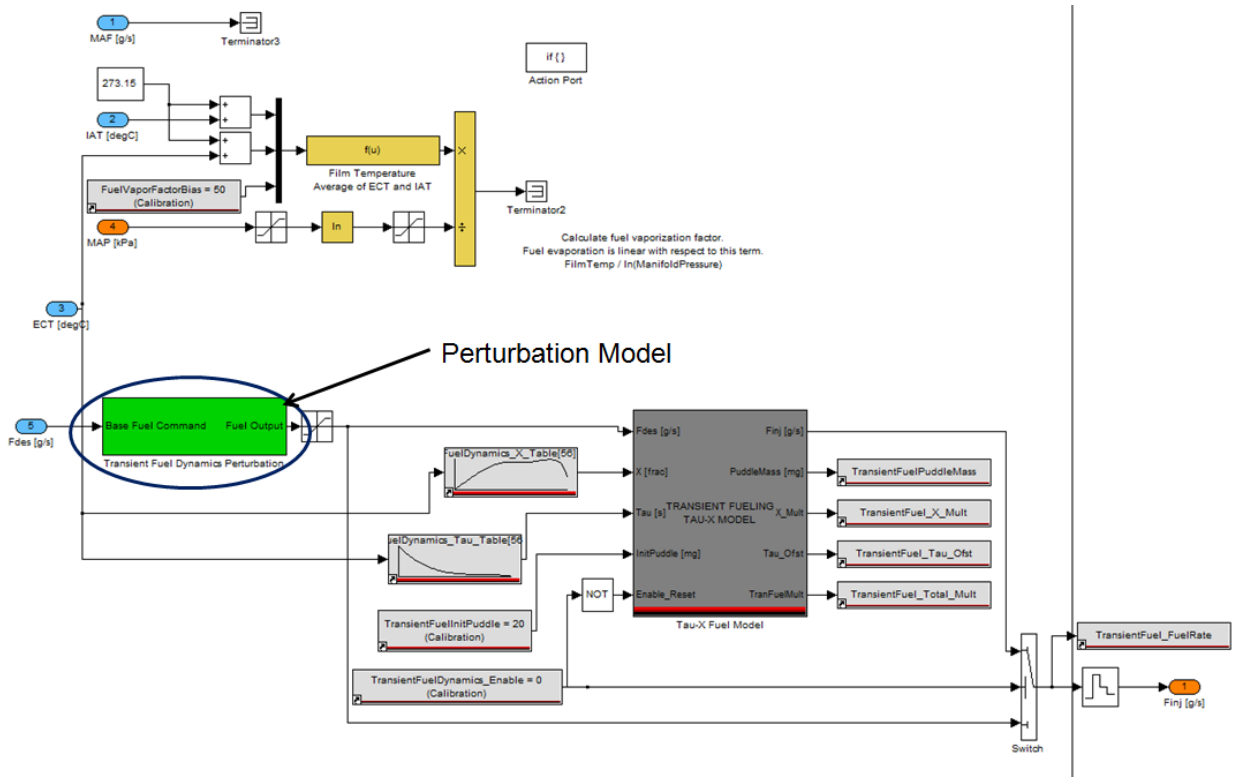

Figure 9:35: Fuel Perturbation Model within Engine Code

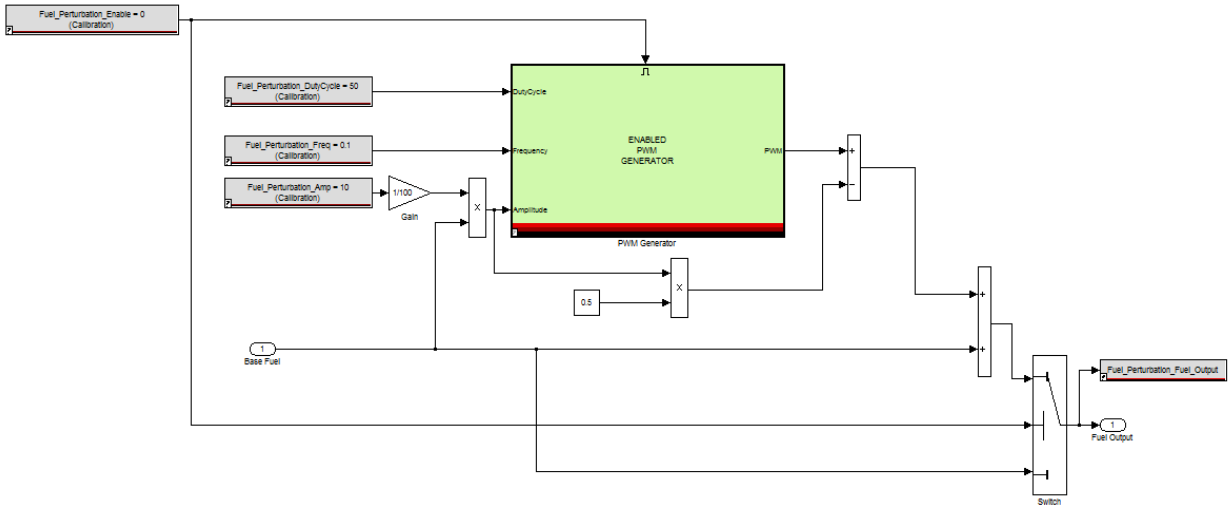

Figure 9:36: Fuel Perturbation Subsystem

APPENDIX B: Selected Figure

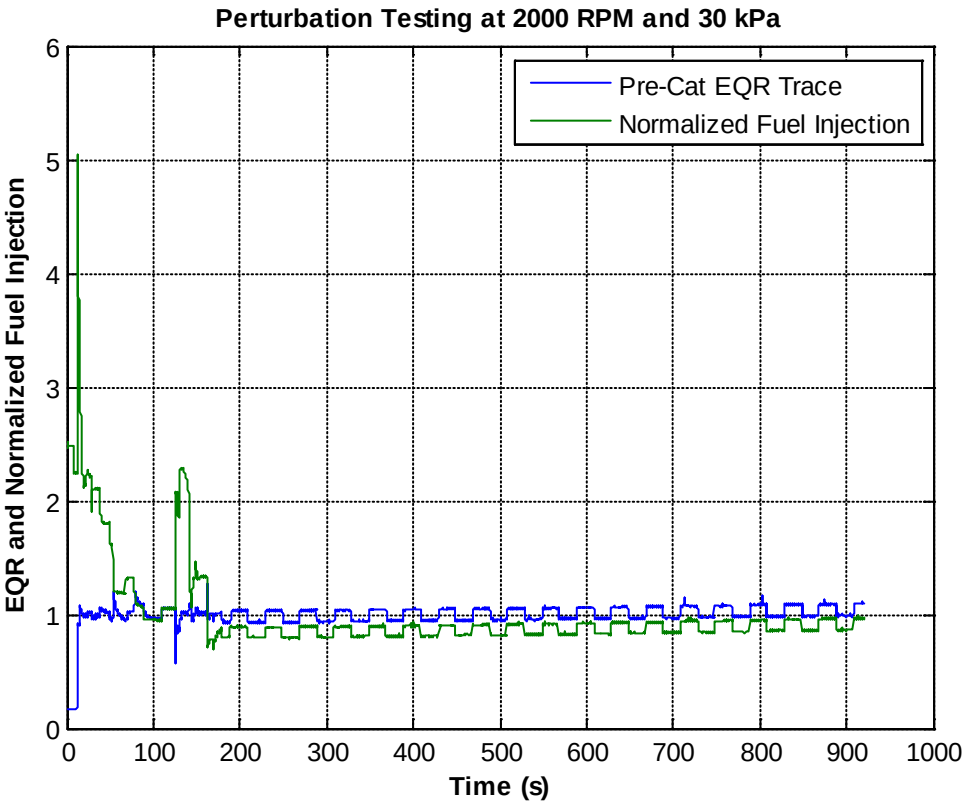

Figure 9:37: Entire Perturbation Test for 2000 RPM and 30 kPa

APPENDIX C: MATLAB Code

Initial τ and X Code

```
clear all
close all
clc

%Load Data
mdfimport('Test_2000RPM_60kPa_27.dat') %import .dat file

EQR_test = PreCatO2_7; %Rename EQR data
time = time_7;


f = 0.5*60000*RunStateFPC__ls_0_rs__8/60000; %Determine rate of fuel entering (mg)-->(g)
f_time = time_8;

MAF = MAF_8;  %rename mass air flow
MAF_time = time_8;
MAF_avg = mean(MAF); %pick later point to calculated MAF

ECT_test = ECT_5; %rename engine coolant temperature
ECT_time = time_5;

%create time vector with 0.007 second intervals
new_time = [0:0.007:time(end)];

%put variables in terms of new time
% for i = 1:length(new_time)
%     fuel_injected(i,:) = interp1(f_time,f,new_time(i));
%     MAF_calc(i,:) = interp1(MAF_time,MAF,new_time(i));
%     EQR(i,:) = interp1(time,EQR_test,new_time(i));
%     ECT(i,:) = interp1(ECT_time,ECT_test,new_time(i));
%     i
% end
%
% save taux_2000_60

%load injected fuel data with 0.007 sec increments
load taux_2000_60

%calculated fuel from EQR
cyl_afr = EQR.*MAF_calc/9.87; %MAF is for all 4 cylinders, so divide by 4

f_size = 1:length(fuel_injected);
c_size = 1:length(cyl_afr);
T_size = 1:length(ECT);

% plot(f_size,fuel_injected,c_size,cyl_afr)
% title('Fuel Rate Injected and Fuel Rate Received by Cylinder')
% ylabel('Fuel Rate (g/s)')
% xlabel('Number')
```

```
% legend('Fuel Rate Injected', 'Fuel Rate Received by Cylinder (AFR)')
% grid on

plot(c_size,cyl_afr)
title('Fuel Rate Received by Cylinder')
ylabel('Fuel Rate (g/s)')
xlabel('Number')
grid on

% %find transport delay between fueling and EQR trace every two pulses
number = 'Number of Good Perturbations = ';
pertnum = input(number) %assign number of up perturbations used

clear time

for i = 1:pertnum
   H = menu('Find Cyl Fuel Pert Start','Select Point');
   [cyl_rise(1,i) ycyl_s(1,i)]  = ginput(1);
   H = menu('Find Cyl Fuel Pert End','Select Point');
   [cyl_end(1,i) ycyl_e(1,i)]  = ginput(1);
end


global X tau %Define X and tau as global variables to use in function and simulink

for i=1:pertnum

   cyl_new = cyl_afr(cyl_rise(1,i):cyl_end(1,i));
   ECT_new = ECT(round(cyl_rise(1,i)):round(cyl_end(1,i)));
   ECT_avg(i) = mean(ECT_new);

   cyl_afr_new = cyl_new-min(cyl_new);  %Adjust AFR fuel from 0 to 1
   cyl = cyl_afr_new/max(cyl_afr_new);

   time = zeros([length(cyl_afr_new) 1]);
   time = 0:0.007:(length(cyl_afr_new)-1)*0.007;
   time_stop = time(end);

   fuel_sim(:,1) = time;

   [n d] = butter(2, .001); %filters normalized afr
   fuel_afr_filt = filtfilt(n, d, cyl);

   fuel_sim(:,2) = fuel_afr_filt(end).*ones([length(cyl_afr_new) 1]);

   B_c = fminsearch(@(x) myfun1(x, fuel_sim, cyl), [.5;6])

   X_new(i) = B_c(1)
   tau_new(i) = B_c(2)

   fuel_cyl_calc = myfun([X_new(i) tau_new(i)], fuel_sim(:,2));
```

```
    figure
    plot(time,cyl,time,fuel_sim(:,2),'-k',  time, fuel_cyl_calc)
    title(['Normalized (EQR), Commanded Fuel Input, and Normalized Estimated Output for Case = ' num2str(i)])
    xlabel('Time (s)')
    ylabel('Fuel Rate (g/s)')
    legend('Normalized EQR','Commanded Input','Estimated Output')
    grid on

    clear cyl_new ECT_new cyl_afr_new cyl time time_stop fuel_afr_filt fuel_sim fuel_cyl_calc  %clear variables
because they change size



end


ECT_avg

figure
plot(ECT_avg,tau_new,'*',ECT_avg,X_new,'*')
title('Tau and X vs. Temp')
```

Second τ and X Code

```
clear all
close all
clc

%Load Data
% mdfimport('Test_4.dat') %import .dat file
%
% EQR_test = PreCatO2_7; %Rename EQR data
% time = time_7;
%
%
% f = 0.5*60000*RunStateFPC__ls_0_rs__8/60000; %Determine rate of fuel entering (mg)-->(g)
% f_time = time_8;
%
% MAF = MAF_8;  %rename mass air flow
% MAF_time = time_8;
% MAF_avg = mean(MAF); %pick later point to calculated MAF
%
% ECT_test = ECT_5; %rename engine coolant temperature
% ECT_time = time_5;
%
% create time vector with 0.007 second intervals
% new_time = [0:0.007:time(end)];

%put variables in terms of new time
% for i = 1:length(new_time)
%     fuel_injected(i,:) = interp1(f_time,f,new_time(i));
%     MAF_calc(i,:) = interp1(MAF_time,MAF,new_time(i));
%     EQR(i,:) = interp1(time,EQR_test,new_time(i));
%     ECT(i,:) = interp1(time_5,ECT_test,new_time(i));
%     i
% end
%
% save taux_2000_60

%load injected fuel data with 0.007 sec increments
load taux_2000_60
load tfit_2000_60

%calculated fuel from EQR
cyl_eqr = EQR.*MAF_calc/9.87; %MAF is for all 4 cylinders, so divide by 4

f_size = 1:length(fuel_injected);
c_size = 1:length(cyl_eqr);
T_size = 1:length(ECT);

% plot(f_size,fuel_injected,c_size,cyl_afr)
% title('Fuel Rate Injected and Fuel Rate Received by Cylinder')
% ylabel('Fuel Rate (g/s)')
% xlabel('Number')
% legend('Fuel Rate Injected', 'Fuel Rate Received by Cylinder (AFR)')
% grid on
```

```
plot(c_size,cyl_eqr)
title('Fuel Rate Received by Cylinder')
ylabel('Fuel Rate (g/s)')
xlabel('Number')
grid on


number = 'Number of Good Perturbations = ';
pertnum = input(number) %assign number of up perturbations used

clear time

for i = 1:pertnum

   H = menu('Start','Select Point');
   [cyl_rise(1,i) ycyl_s(1,i)]  = ginput(1);
   H = menu('UP','Select Point');
   [cyl_up(1,i) ycyl_up(1,i)]  = ginput(1);
   H = menu('DOWN','Select Point');
   [cyl_down(1,i) ycyl_down(1,i)]  = ginput(1);
   H = menu('End Total','Select Point');
   [cyl_end(1,i) ycyl_e(1,i)]  = ginput(1);
   H = menu('Steady State Value 1','Select Point');
   [cyl_ss1(1,i) ycyl_ss2(1,i)]  = ginput(1);
   H = menu('Steady State Value 2','Select Point');
   [cyl_ss2(1,i) ycyl_ss2(1,i)]  = ginput(1);
   H = menu('Start Avg Value 1','Select Point');
   [cyl_st1(1,i) ycyl_st2(1,i)]  = ginput(1);
   H = menu('Start Avg Value 2','Select Point');
   [cyl_st2(1,i) ycyl_st2(1,i)]  = ginput(1);
end


global X %Define X as a global variable to use in function and simulink

for i=1:pertnum

   cyl_new = cyl_eqr(cyl_rise(1,i):cyl_end(1,i));
   ECT_new = ECT(round(cyl_rise(1,i)):round(cyl_end(1,i)));
   ECT_avg(i) = mean(ECT_new);


%%%    for initial steady state value (set to 0)

   start = cyl_st1(1,i)-cyl_rise(1,i);
   last = cyl_st2(1,i)-cyl_rise(1,i);

   cyl_eqr_new = cyl_new-mean(cyl_new(start:last));  %Drops to

%%%    for final steady state value (set to 1)

   start = cyl_ss1(1,i)-cyl_rise(1,i);
```

```
    last = cyl_ss2(1,i)-cyl_rise(1,i);

    cyl = cyl_eqr_new/mean(cyl_eqr_new(start:last));

    time = zeros([length(cyl_eqr_new) 1]);
    time = 0:0.007:(length(cyl_eqr_new)-1)*0.007;
    time_stop = time(end);

    fuel_sim(:,1) = time;

    fuel_sim(1:cyl_up(1,i)-cyl_rise(1,i),2) = 0;
    fuel_sim(cyl_up(1,i)-cyl_rise(1,i):cyl_down(1,i)-cyl_rise(1,i),2) = 1;
    fuel_sim(cyl_down(1,i)-cyl_rise(1,i):cyl_end(1,i)-cyl_rise(1,i),2) = 0;

    tau(i) = a*ECT_avg(i)^b+c;

    B_c = fmincon(@(x) mymult_X(x, fuel_sim, cyl), [.6],[],[],[],[],[0.01],[0.99])

    X_new(i) = B_c(1)


    fuel_cyl_calc = mytau([X_new(i)], fuel_sim(:,2));

    figure
    plot(time,cyl,time,fuel_sim(:,2),'-k',  time, fuel_cyl_calc)
    title(['Cylinder Fuel (EQR) vs. Calculated Cylinder Fuel (Fuel Injected/Fit) for Case = ' num2str(i)])
    xlabel('Time (s)')
    ylabel('Fuel Rate (g/s)')
    legend('filtered measured output','commanded input','estimated output')
    grid on

    clear cyl_new ECT_new cyl_eqr_new time_stop x  fuel_cyl_calc  %clear variables because they change size
    clear fuel_new inj_new time  fuel_sim
    clear fuel_new


end



ECT_avg

figure
plot(ECT_avg,tau,'*',ECT_avg,X_new,'*')
title('Tau and X vs. Temp')
legend('Tau','X')
```

Appendix D: Simulink Models

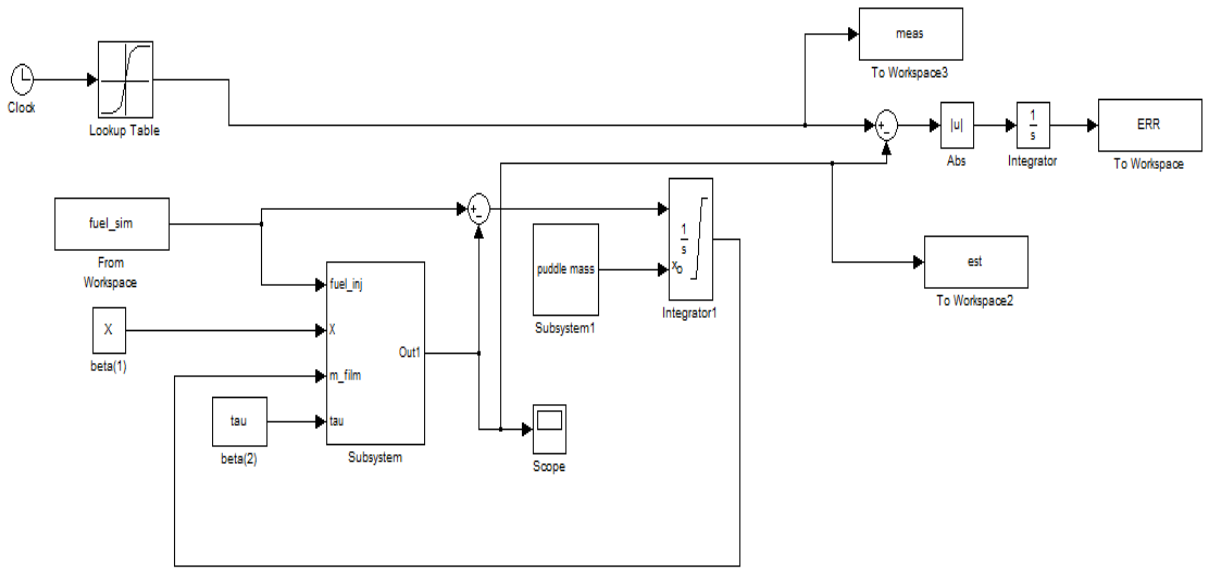

Figure 9:38: 1st Fuel Dynamics Simulink Model for Initial Method

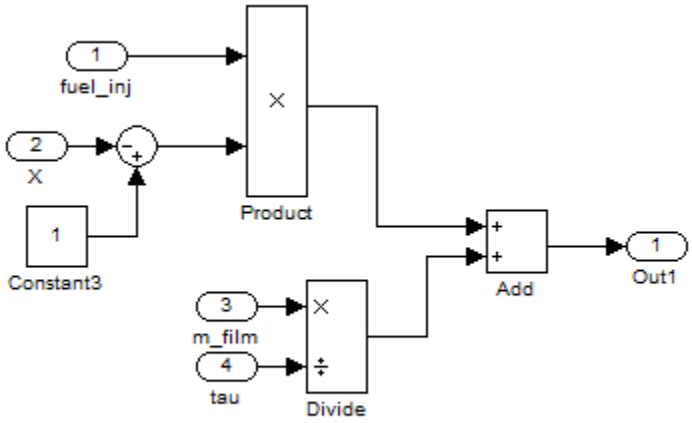

Figure 9:39: Simulink Model's Fuel Dynamics Subsystem

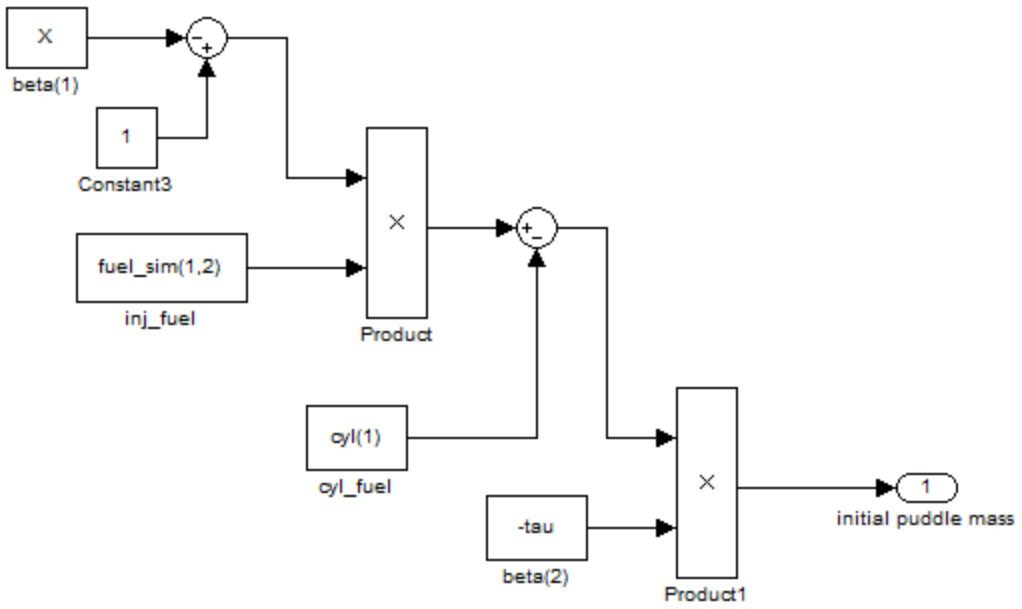

Figure 9:40: Simulink Model's Initial Fuel Puddle Subsystem

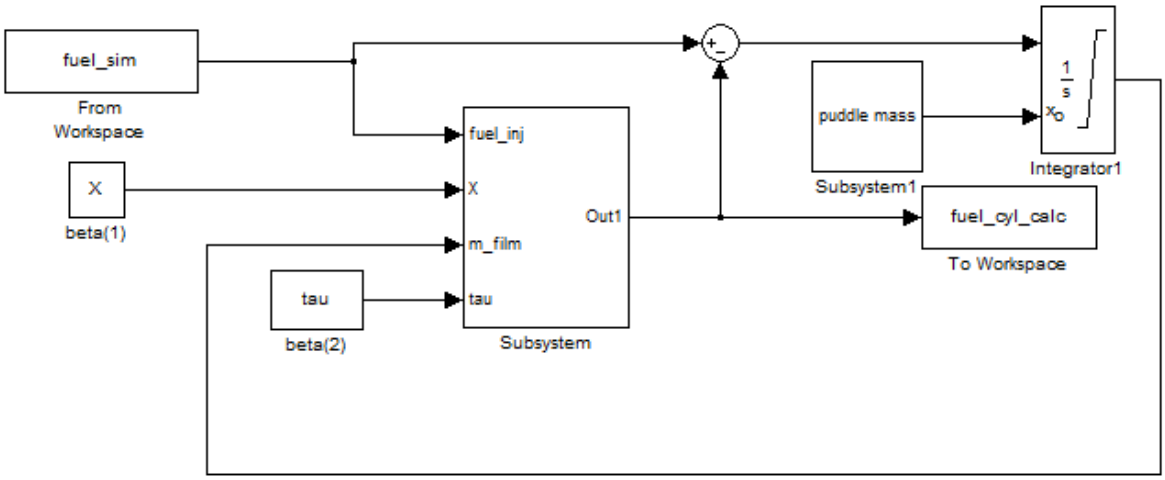

Figure 9:41: 2nd Fuel Dynamics Simulink Model for Initial Method

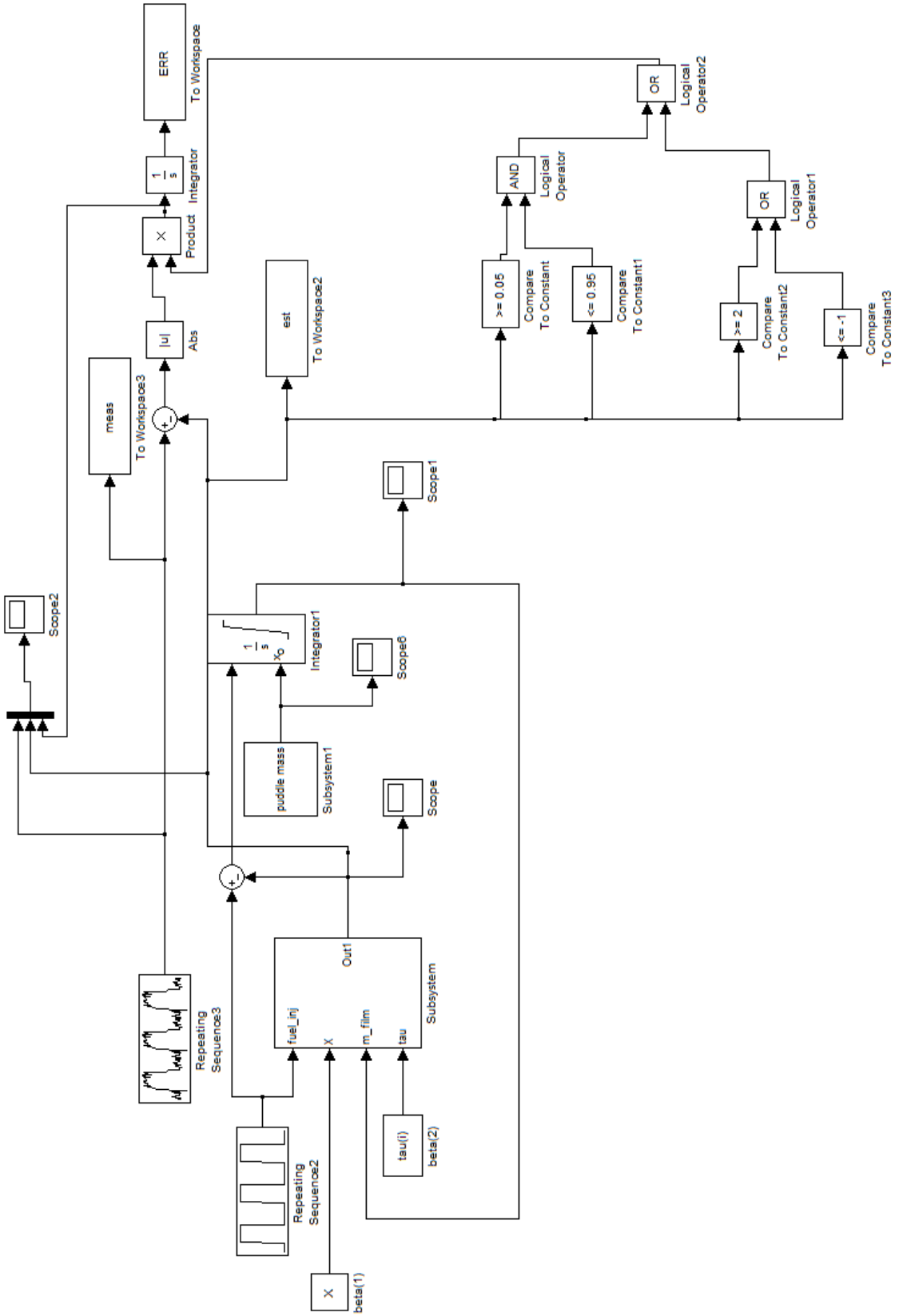

Figure 9:42: Updated Simulink Model for Second Method

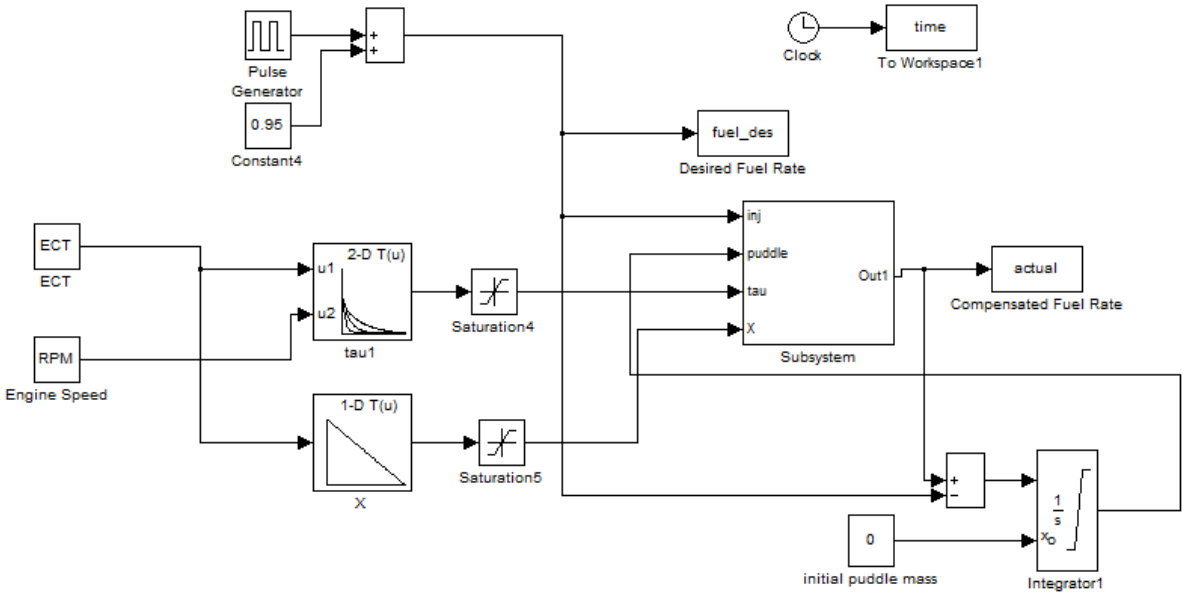

Figure 9:43: Simulink Fuel Compensator Algorithm

Appendix E: Curve Fits

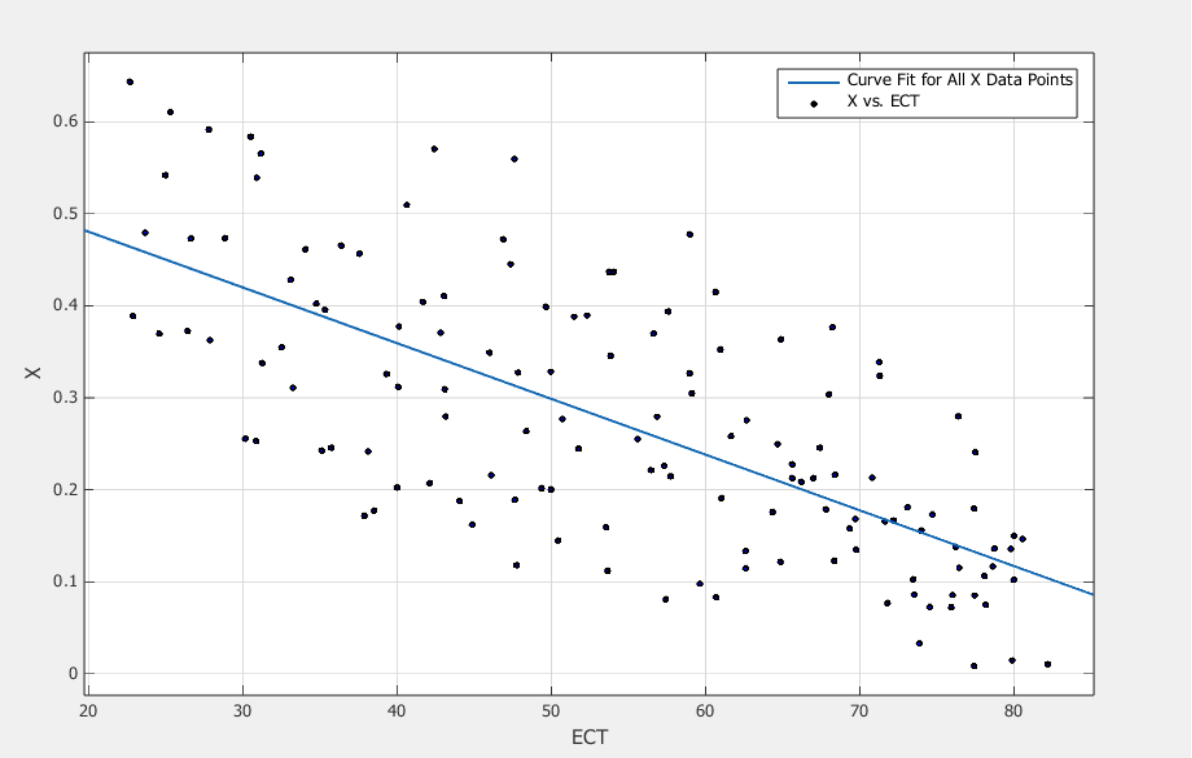

Figure 9:44: Curve Fit of All X Data Points

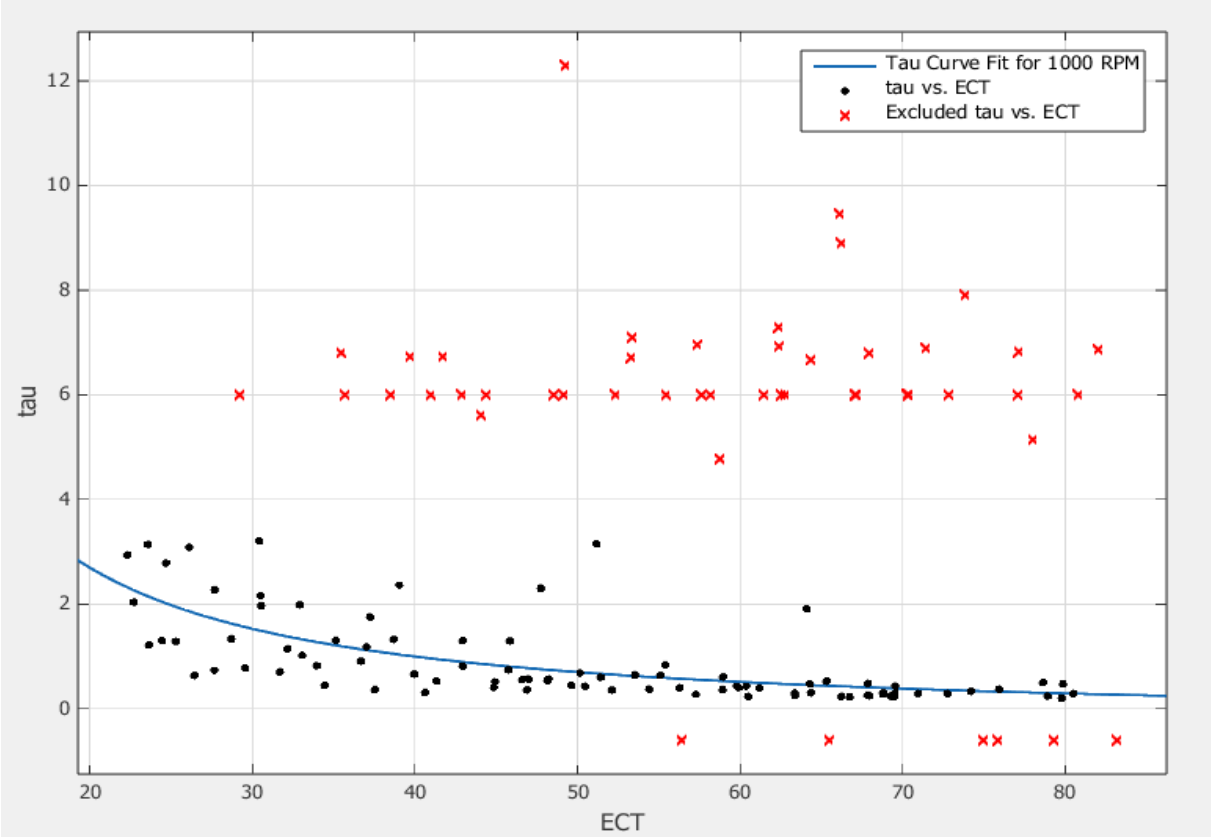

Figure 9:45: Curve Fit of τ for 1000 RPM

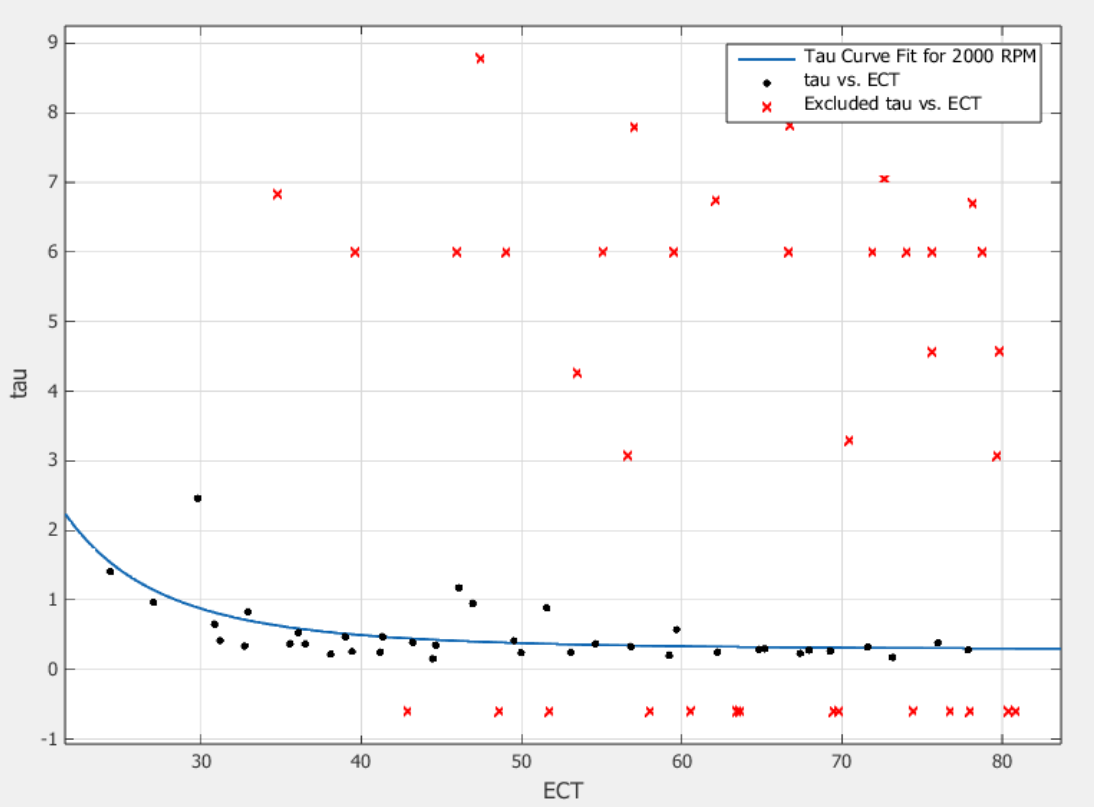

Figure 9:46: Curve Fit of τ for 2000 RPM

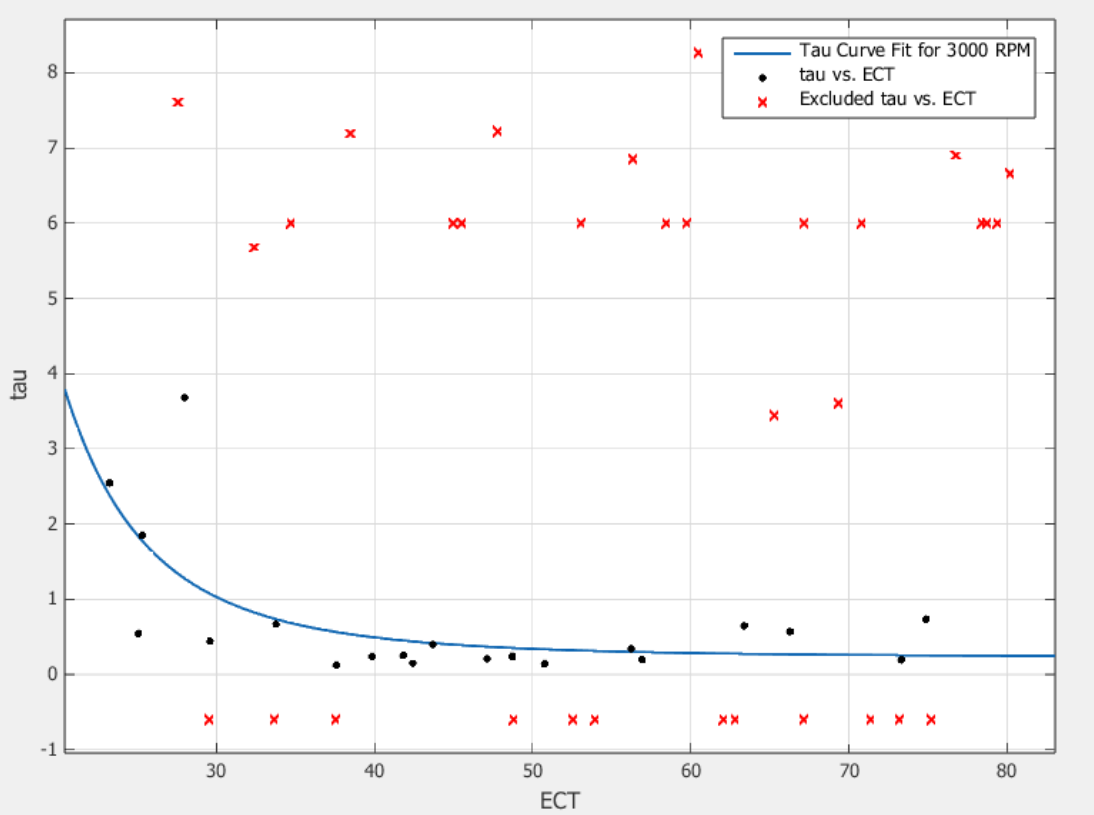

Figure 9:47: Curve Fit of τ for 3000 RPM